EFFORTE –

'Efficient forestry by precision planning and management for sustainable environment and cost-competitive bio-based industry'

This project has received funding from the Bio Based Industries Joint Undertaking under the European Union's Horizon 2020 research and innovation programme under grant agreement No 720712
Project duration: 1.9.2016–30.8.2019.
Coordinator: Natural Resources Institute Finland (Luke).

Deliverable 3.5 – Logging trail visualizations and post-harvest quality control		
Work Package 3 - Big Data bases and applications		
Task 3.5- **Logging trail visualizations and post-harvest quality control**		
Due date	31.08.2018	
Author(s), organisation(s)	Erik Willén (Skogforsk), Patrik Flisberg, Mikael Frisk (Creative Optimization), Jari Ala-Ilomäki, Harri Lindeman, Aura Salmivaara (LUKE), Heikki Ovaskainen (Metsäteho)	
Date of publication	31.08.2018	
Dissemination level		
PU	Public	X
PP	Restricted to other program participants (including the Commission Services)	
RE	Restricted to a group specified by the consortium (including the Commission Services)	
CO	Confidential, only for members of the consortium (including the Commission Services)	
Nature of the Deliverable		
R	Report	R
P	Prototype	
D	Demonstrator	
O	Other	

Table of contents

1. EFFORTE project objectives

EFFORTE is a research and innovation project providing the European forestry sector with new knowledge and knowhow that will significantly improve the possibilities of forest enterprises to assemble and adopt novel technologies and procedures.

The project aims at enhancing the efficiency of silviculture and harvesting operations; increasing wood mobilization and annual forest growth; increasing forest operations' output while minimizing environmental impacts; and reducing fuel consumption in the forest harvesting process by at least 15%.

The project is based on three key elements of technology and knowhow:

1) Basic understanding of fundamentals of **soil mechanics and terrain trafficability** is a crucial starting point to avoid soil disturbances, accelerate machine mobility and assess persistence of soil compaction and rutting. The key findings and recommendations of trafficability related to EFFORTE can immediately be adapted in all European countries.

2) Due to decreasing Cost-competitiveness of manual work and maturity of technology it is now perfect time to realize the potential of **mechanization in silvicultural operations**. EFFORTE pursues for higher productivity and efficiency in silvicultural operations such as tree planting and young stand cleaning operations.

3) 'Big Data' (geospatial as well as data from forestry processes and common information e.g. weather data) provides a huge opportunity to increase the efficiency of forest operations. In addition it adds new possibilities to connect knowledge of basic conditions (e.g. trafficabillity), efficient silviculture and harvesting actions with demand and expectations from forest industries and the society. Accurate spatial information makes it possible for forestry to move from classic stand-wise management to precision forestry, i.e. micro stand level, grid cell level or tree-by-tree management. EFFORTE aims at achieving substantial influence to the **implementation and improved use of Big Data within Forestry** and through this increase Cost-efficiency and boost new business opportunities to small and medium size enterprises (SME) in the bioeconomy.

EFFORTE researchers will develop and pilot precision forestry applications that, according to the industrial project partners, show the greatest potential for getting implemented immediately after the project.

2. Logging trail visualizations and post-harvest quality control

To reduce the impact on forest soils the EFFORTE project develop and refine trafficability maps to be used in forest planning and operations as reported in Efforte reports D3.3 and D3.4. In addition to the trafficability maps, further forest operator tutoring systems are essential for operational implementation of tools and methods to reduce negative impact on water and soils.

The first two sections of this report include similar methods to find and describe best harvesting and forwarding routes. A decision support tool can be developed based on algorithmic methods using terrain and water models (DTM and WAM based on LiDAR scanning), predicted product yield combined with information on restricted areas due to cultural- and natural heritage and suggested landing sites at roadside. This could have a significant impact on the productivity and environmental considerations in forest operations. Shorter forwarding distance may be achieved taken the terrain and water models in consideration to avoid severer rutting.

This report also includes two pilot operator tutoring systems that in addition to WAM help forest machine operators and forest managers to prevent soil damages. Knowing soil bearing capacity is one key factor for harvesting operations, especially for the loaded forwarder, following the trail of the lighter harvester.

A harvester was equipped for autonomous collection of data from the transmission CAN-bus for modelling detection of soil bearing capacity. Furthermore, a quality control tool was constructed based on industrial 2-D laser scanner data to automate post-harvest quality assessment and replace point-wise data with continuous recording. The post-harvest quality variables measured with the laser scanner included rut depth and logging trail width. In addition to quality assessment, the data on soil properties can be used in other applications.

This report includes four sections:

1. Methods to plan logging trails to prevent soil damage using Big Data, the Bestway model
2. Methods to plan logging trails to prevent soil damage using Big Data, the Ajourakone model
3. Methods for using forest machine data (transmission CAN-bus) for modelling soil bearing capacity in logging trails
4. Methods for using industrial 2-D laserscanner mounted on forest machine to automate post-harvest quality assessment of rut depth

The report focuses on method development and initial testing while validation plans is described and results from the validation to be further reported in Efforte report D 4.5.

3. Main extractions routes planning – The Bestway Model

Introduction

During 2015 Skogforsk conducted a survey concerning operational forestry planning at seven forest companies in Sweden (Willén & Andersson, 2015).

The survey revealed that the planning prior to forest operations is crucial to comply with the requirements on productivity and quality of the operations, but also requirements to fulfil environmental considerations and cultural heritage. The planning also includes silviculture procedures and forest road maintenance. As forest operations and logistics is about 80% of the costs in forestry the forest planner performance is of high importance for all forest operations.

The recent evolution of Big Data and especially LiDAR applications such as digital elevation models (DEMs), forest estimates and depth-to-water(DTW) maps has been a leap for the forest planner and the ability to perform the tasks efficiently. The study however suggest that the planning effort could be even more rationalized, e.g. by performing even more planning indoors prior to field checks and simplifying the administrative routines for production of cutting directives.

Water and forest operations

During the last years the problems with rutting from forest machines and its impact on streams or other water courses have been in focus. In Sweden a common policy for soil and ground damages in forestry have been established also classifying different ruts or other damage caused by forest machines (Berg et al, 2010).

Studies have shown that more ruts are found on wet or moist soils, while damage on dryer soils are limited (Bergkvist et al., 2014; Friberg & Bergqvist, 2016). By concentrating log extraction to soils with better bearing capacity and put slash from trees (tops and branches) in the extraction route and complement with temporarily passages and simple bridges in wet areas it is possible to reduce the damage to the soil from forest machines.

Digital terrain models and depth-to-water maps

A new national DEM, covering Sweden, derived from LiDAR have been a break for the forestry planning both utilising the detailed topography, but also the possibility to produce forest estimates when combining the LiDAR data with sample plots from the national forest inventory.

DTW-maps developed by University of New Brunswick (Bergkvist et al., 2014) model the distance to ground water based on height and slope conditions in the terrain compares to the surroundings have been introduced at all forest companies and is also commonly used in forestry planning (figure 1). Skogforsk has refined this methodology.

Figure 1. DTW maps on orthophoto where bluish areas indicate ground water within 1 metre and d ark blue areas are ground water close to the surface according to the model

Validation of the DTW-maps show the potential to reduce the most severe driving damage by avoiding terrain transportation in the areas where the model finds ground water close to the surface (Friberg & Bergqvist, 2016). The mapping of soil moisture fits well compared to field measurements (Bergkvist et al., 2014).

SPORRE

Skogforsk has developed an optimization tool for terrain transportation during forest operations, SPORRE (Jönsson et al., 2011). It is a route optimization tool for forwarding operations. By using information on the harvester route and cut forest volumes it is possible to optimize the forwarding operations. The model suggested alternative forwarder routes to minimize the total length of log extraction. Input data to the model included the harvester production files. The results were presented as nodes which the forwarder should pass and in what order. At each node the piles to load was presented together with weight and volume.

STIG

In the STIG-project Skogforsk has since 2010 developed and refined decision support for forestry planning and operations (Bergkvist et al., 2014). As described the new national DEM with a 2-metre spatial resolution has been a key to success as the previous DEM had a 50-metre resolution. By using the DEM and DTW-maps more than 100 training workshops been held to introduce the decision support to almost all forest planners and harvester teams in Sweden. Further development could include models to suggest main extraction roads together with existing decision support.

Aim and objectives

Based on the experiences from the STIG- and SPORRE projects a need for decision support for main extraction routes for the forwarder was identified. The concept was called *Bestway* and should suggest main extraction routes prior to field planning by the forest planners.

Objectives:

- Develop a model that use DEM, DTW and data describing the forest to optimize the layout of main extraction routes and deliver key figures for the forwarding operation enabling scenario modelling.

The aim within EFFORTE project was to refine and validate the model in operational conditions at a forest company.

Material and methods

The model

The perform an optimization data for calculations as well as user defined data are required. The data for calculations cover the full area of the forest stand and surroundings while user defined data complement and may be collected in field. To suggest terrain transportation routes, a model should include the topography (to avoid steep areas), DTW-maps (to avoid wet areas) and variations in forest volume (to steer the forwarding route). It should be complemented with "No GO" areas where no terrain transportation should take place. A general specification:

- **Data for calculations**
  - A detailed DEM
  - DTW-maps
  - Forest volume in raster format to capture variations within the forest stand
  - No Go areas (E.g. nature reserves or cultural heritages)
- **User defined data**
  - Landings
  - Boundaries for the proposed final felling
  - Possible passages, e.g. for water courses
  - Potentially new environmental considerations

The optimization model in Bestway balances two different goals:

- Shortest driving time to forward the timber.
- Location of the forwarding routes with regards to nature values, wood volume, soil and water.

The goals can coincide (but do not need to) and the mathematical model that can be used to solve this problem is closely related to a network design problem (Lundgren et al., 2010).

The optimization is performed on a 3 x 3-pixel raster data of the area. Each pixel is modelled as a node and from each node there are links to each of the eight adjacent nodes. There are restrictions on where to drive, which may cause all eight links not always being included in the optimization. Each link consists of two arcs representing the two directions of the link. Figure 2 illustrates a section with 16 pixels represented as nodes with links between them.

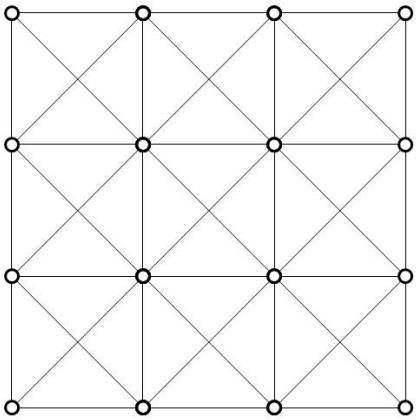

Figure 2. Illustration of a discretization of an area which is represented by a network.

The pixel size of 3 × 3 meters was determined as the width of a forwarder or harvester is roughly three meters and each pixel then corresponds to the width of the machine.

Wood piles are generated in areas where there is forest (according to the input forest estimates) and they are distributed in a way that all trees can be reached with a forwarder from (at least) one wood pile. The nodes that are associated to pixels where there are wood piles are called supply nodes. The demand nodes consist of the landings. All the wood volumes are to be transported in the network from the supply nodes to any of the demand nodes. This corresponds to the flow in the network.

Each node is linked to real terrain predefined in raster data via coordinates. The input consists of a cost index surface given as raster data. The cost index surface value is based on the time it takes to drive (depending on for example slope). The arc costs are associated with the value of the cost index surface between the nodes they run. It may also include a penalty if the surface is in a place where driving should be avoided (No Go areas, damp and wet areas, etc.).

Figure 3 and Figure 4 show how the model works on an example with 6 supply nodes (wood piles) and a demand node (landing).

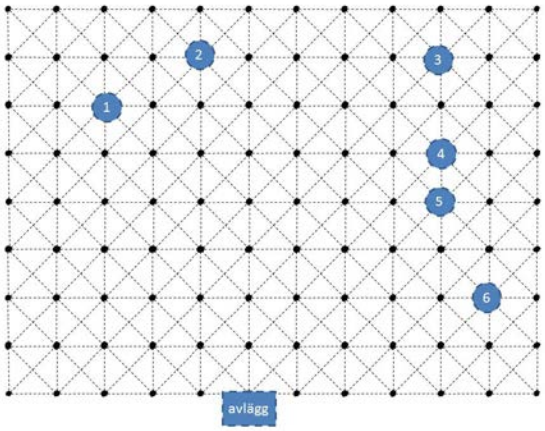

Figure 3. An illustrative example with six supply nodes (wood piles) and one demand node (landing).

With appropriate levels of fixed and variable costs on links, the model could provide the solution in which the thickness of the links corresponds to the size of the flow. Both the flow cost and the cost of using links are minimized.

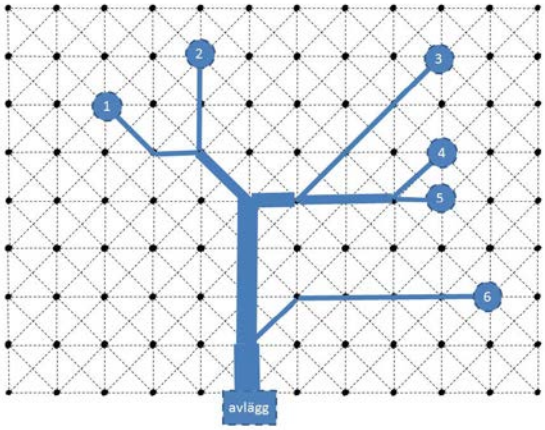

Figure 4. Solution to the illustrative example with six supply nodes and one demand node (landing).

A Lagrange heuristic solution method was used to solve the optimization problem for the presented model. It is based on Lagrange relaxation and subgradient optimization (Lundgren et al., 2010). Some constraints were relaxed, and the remaining problem was relatively easy to solve. When using subgradient optimization, errors in the relaxed constraints are penalized in an iterative process to converge to a solution that corresponds to the model's optimal solution.

In the study, the constraints that linked the flow in the network with different flow levels were relaxed. After relaxing these constraints, the problem could be divided into two sub problems:

1. Finding the cheapest route between each supply node and each demand node.

2. To calculate a reduced cost for each arc which is used to determine the maximum allowed flow level on each arc.

Sub problem 1 could create several parallel routes with were located too close to each other, which is not effective from a practical logistic perspective. The subgradient methodology then punished such solutions and instead favored solutions with a fewer number of used arcs, which aimed at creating only one route instead of several parallel ones.

After several iterations a good solution was computed and using the example problem above from Figure 3 and 4 we get the solution in Figure 5 (after a practical adaption of the model).

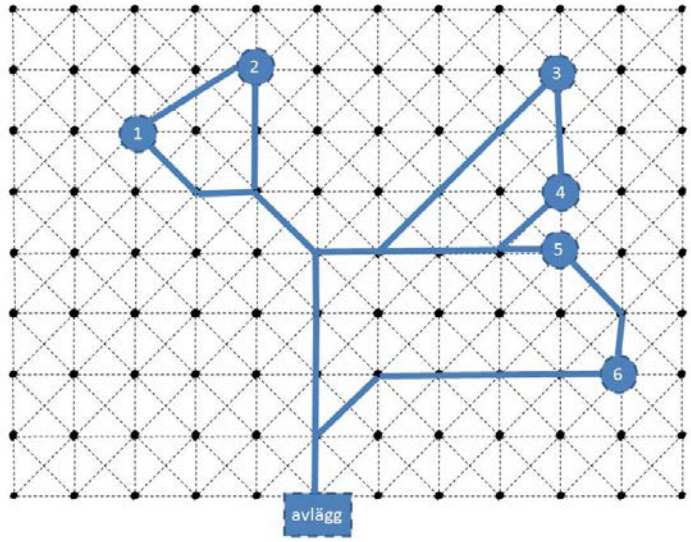

Figure 5. Illustration of a solution where the practical requirements are met simultaneously.

To calculate mileage, time and other relevant key number given the optimized road network, the methodology from SPORRE (Flisberg, et al., 2007) was used.

The model implementation, shown in figure 6, produces main extraction routes from the landing by the forest road to the final felling. The suggested extraction route uses a forest stand delineation and landing position proposed by the user. In the model an optimization is performed using DEM, DTW-maps, forest volume estimates and known environmental considerations and cultural heritages (No Go areas).

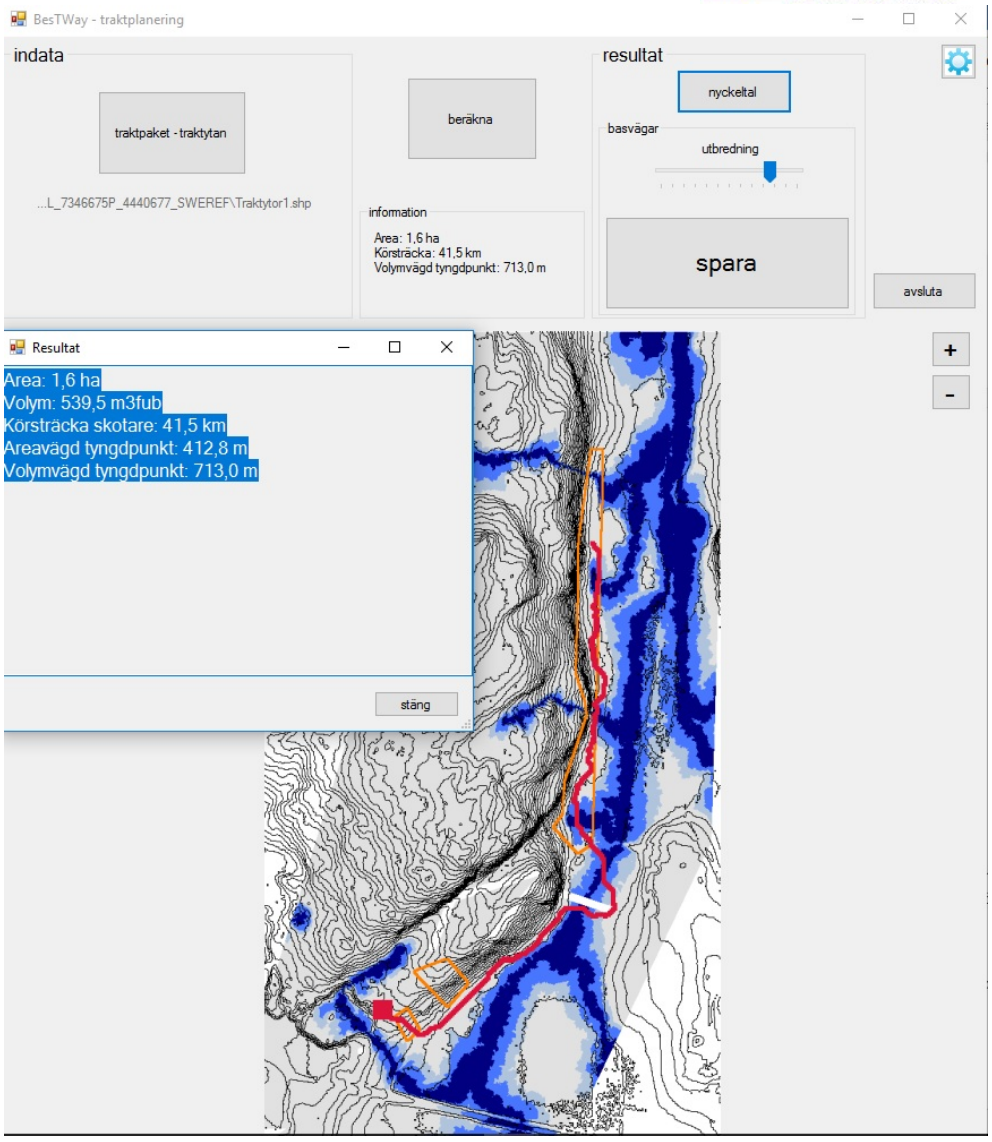

Figure 6. Bestway model. Main extraction route is shown as a red line.

Model testing

The Bestway model was tested within the Sollebrunn forestry district at the forest company Södra, figure 7, located in western part of Sweden. Södra is an economic association with about 50 000 members, private forest owners in the southern part of Sweden.

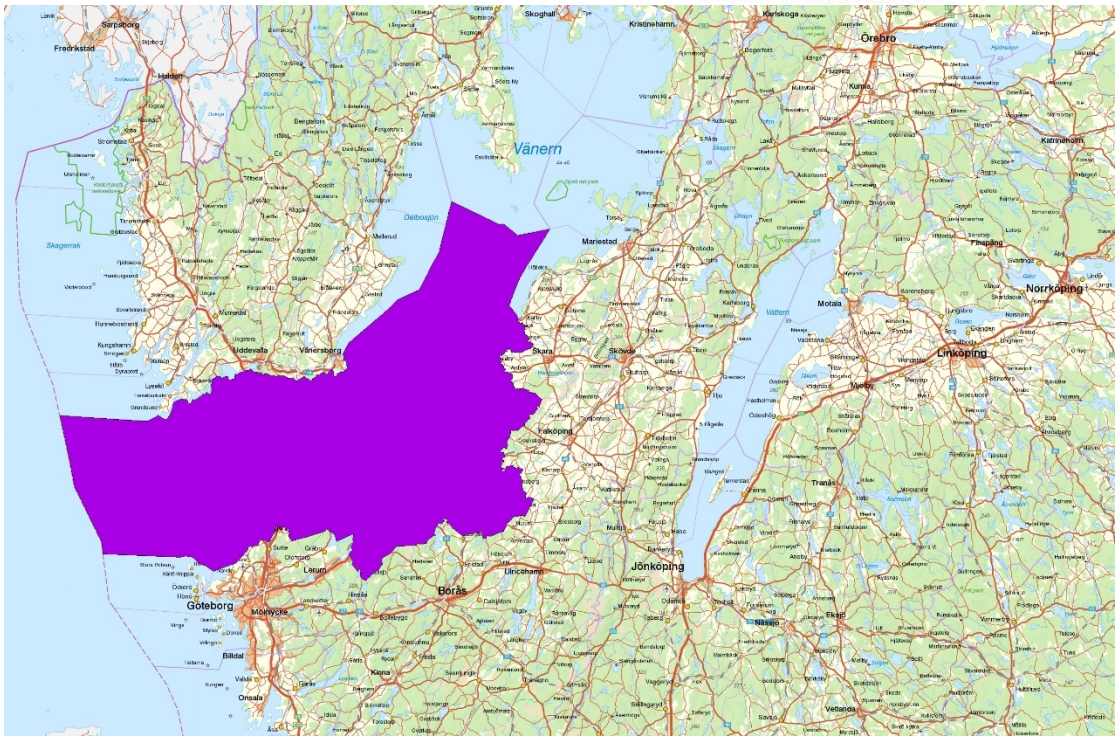

Figure 7. Sollebrunn forestry district in purple. © Lantmäteriet.

Data for calculations in the model:

- Grid 2+,
  Dem from Lantmäteriet, 2 metre spatial resolution

- DTW-maps,
  DTW-maps with four thematic classes, 0-0,25 metre;0,25-0,5 metre; 0,5-1 metre; > 1 metre to ground water. 2 metre spatial resolution.

- Forest volume estimates
  Forest volumes derived from LiDAR and national forest inventory, freely available from the Swedish Forest Agency, raster 12,5 metre spatial resolution.

- No Go areas
  No Go areas including environmental considerations from Swedish Environmental Protection Agency, Swedish Forest Agency and The Swedish National Heritage Board.

The user defined data as landing sites and forest stand boundaries were collected from the Södra GIS system. 18 planned final fellings was used for the testing and their size varied from 0,6-8 hectares with estimated forest volumes of 168-2142 cubic metres.

Method

Forestry professionals from Södra were included in the study. Already planned final fellings were used and the Bestway model applied. The key figures were documented and compared to the figures from the planning process.

The Bestway model was used for 18 cuttings, checked in field inspections prior to forest operations and then used by the harvester team. To discuss the test results a workshop were held with Skogforsk, Södra forestry professionals (both local and central staff) and the harvester team. A broad perspective on the use of the model was addressed during the workshop.

Results

Mean forwarding distance was estimated in 15 of the 18 cuttings by forestry professionals. 10 out of 15 had a shorter mean forwarding distance provided by the Bestway model. In two of the cuttings with shorter estimated forwarding distance the difference was due to possibilities to use passages over water streams and error in DTW-maps that explained the model providing longer distances.

As the total forwarding distance (according to the model) varied from 9,1-164,5 kilometres, any shortening of the forwarding distance will increase the productivity.

The forestry professionals found the mean forwarding distance useful to consider in the dialogue with the harvester teams as the distance is part of the compensation. They also found the Bestway model very useful for new forestry professionals with limited experience in where to put the main extraction routes. Figure 8 shows an interesting example of the full route network and where the extraction route from the landing to the final fellings passes through young forest. This could be a good idea that is normally not considered, without the model result. Most often the forwarding route is kept within the felling site although it may provide longer forwarding distances.

One challenge is the fact that Södra sometimes have very small final fellings where the harvester team needs to stick within the property of the land owner and that could limit the possibilities to pass on the shortest and most efficient route to the final felling. In many cases there are also old routes that the forest owner wants Södra to use, often in-optimal.

As the topography in Sollebrunn forestry district is rather hilly the forestry professionals also tested the possibility to adjust the accepted slope parameters in the model (accepted slope in percent for the forwarding operations) but found the default parameters acceptable also in their hillier region.

Figure 8. Full forwarding network with the route from the landing to the site crossing younger forest.

During the workshop an ongoing forest operation was visited, figure 9. The use of the model was then discussed with both forestry professionals and the harvester team, including forwarder, performing the operation.

During the discussions several of the operational benefits with the model was identified. The harvester team thought that the model results provided useful results in about 7 out of 10 sites and then provided support for the planning of the extraction routes. Several activities in their operation could be rationalized, especially where to start the harvesting as they normally start harvesting along the stand boundaries, but now could start immediate in the stand. They also found it reassuring that the model included the data they usually need to consider. As the model provides the main extraction routs they could also start putting tops and branches in the route to minimize the damage to the ground. The harvester can identify where most of the terrain transportation of wood will appear and may put some extra tops and branches at suitable locations along the route for the forwarder to fill in.

The forestry professionals and the harvester team though that the model probably was most useful in cuttings larger then about three hectares and could play in essential role also for more unexperienced operators to support their route planning.

When starting the operations in figure 9 the northern part was excluded from the cutting, then if the model could be used again with these changes it could be highly useful. It is rather common that there are changes from the original planning when it comes to size of the planned cutting.

In summary the model results provided better results than initially expected and that most suggested main extraction routes could be used during forest operations. The possibility to be able to modify for example stand boundaries and run the model again was desirable.

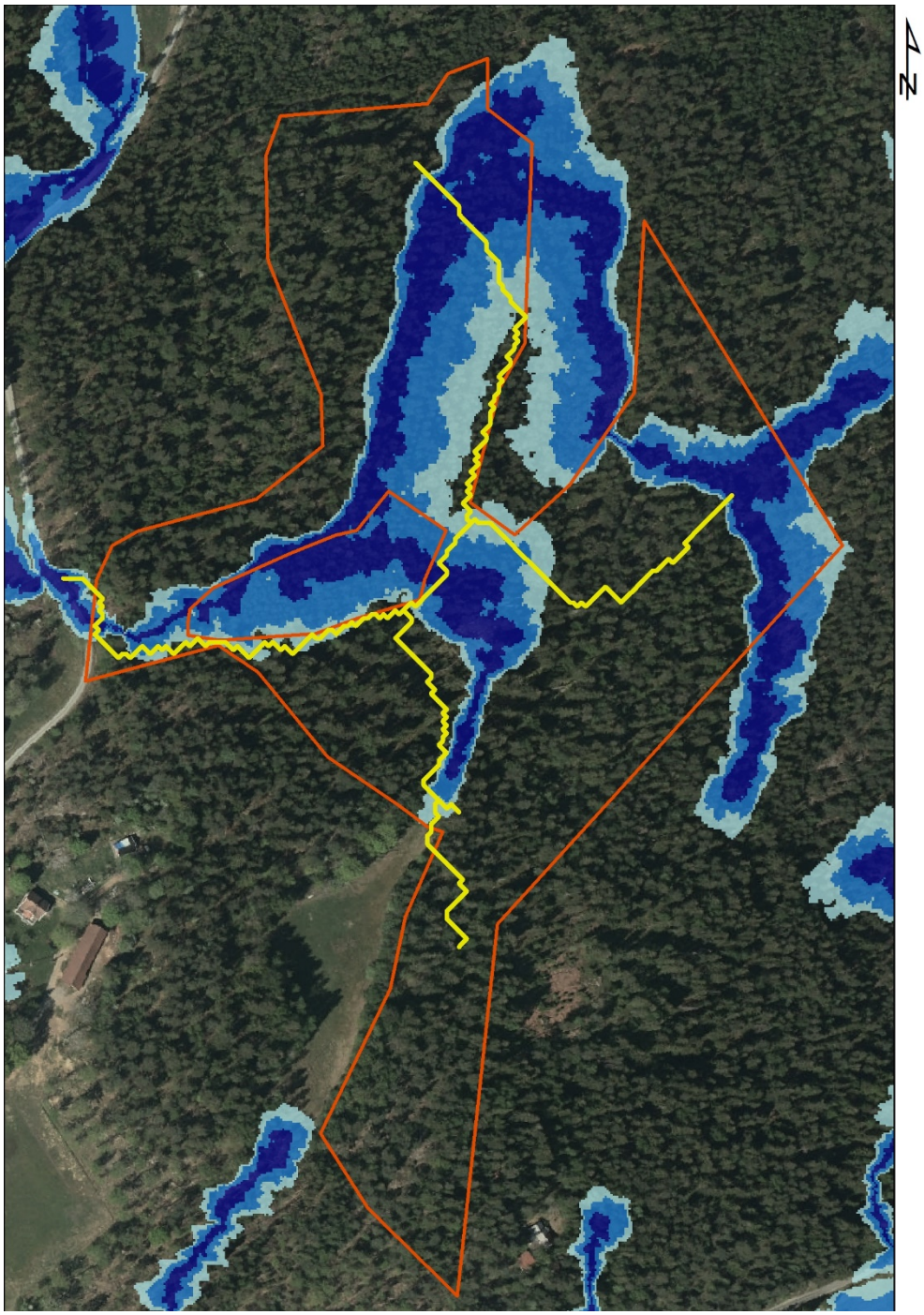

Figure 9. Orthophoto including Bestway model results (yellow) start from the landing to the left in the figure. Bluish areas are the DTW-map and red line the stand boundary.

Discussion

The input data from Södra to the model was successfully implemented. The model uses a thematic DTW-map while Södra had a continuous version, but possible to adjust. This may be changed in coming versions of the model. Most important was the fact that the DTW-maps at Södra was possible to use for digital analyses as some other companies have versions only for visual interpretation. Concerning the No Go areas relatively few were included in the digital layer, so any additional consideration needs to be complemented by the user during modelling.

To ease the use of the model user defined input data was imported in Södra format, however as this format changes now and then further changes in in model will be required. It is also important to easy add or remove landings, passages or additional considerations to test different scenario with the model

During the testing several benefits with the model were identified:

- Main extraction routes taking topography, soil moisture, forest volume and considerations into account

The testing indicated main extraction routes from the model close to where it should have been put by forestry professionals. They, as well as harvester teams, found the model results useable in operations, but also knew that it is a suggestion not possible to use everywhere. It was an excellent starting point. Already during the testing, the direct use of the routing was preferred for the harvester rather than the normal starting route along the stand boundaries.

- Scenario analyses with different landings, passages or additional considerations

The scenario analyses option was interesting, but difficult to implement in the IT-system provided by Södra currently. Its normally not done but seemed to be an interesting tool to use together with the land owner to discuss different routes also passing in younger forest or on another landowner property. If the reduction of forwarding distance is substantial it might be possible to compensate other landowners passing their property.

- Increased efficiency in the dialogue with harvester teams

By using the Bestway model the dialogue with forest professionals and harvester team be more efficient. Scenarios may be modelled and the mean forwarding distance calculated and not estimated.

- Mean forwarding distance calculated in same way

The Bestway model provides mean forwarding distances to be used in the contracts with the harvester teams. This was tested, but not validated in operational use. The main advantage for Södra would be a more objective method to calculate mean forwarding distance and to reduce the variation caused by estimations by different forest professionals at Södra.

Plans for validation

This testing was performed during 2017 in a forestry district, Sollebrunn, with only one harvester team and one forest professional. For 2018 a validation exercise is planned with three forestry districts and at least three professionals at each district providing hopefully more than 100 final fellings modelled by Bestway. That will ensure to capture the variations all over Södra areas, southern Sweden, and a wider use of forest professionals to identify both benefits and challenges. In additions the Bestway model will be tested in Finland.

References

- Berg, R., Bergkvist, I., Lindén, M., Lomander, A., Ring, E. & Simonsson, P. 2010. A proposal for a common policy regarding driving damage in Swedish forestry. Skogforsk. (In Swedish)
- Bergkvist, I., Friberg, G., Mohtashami, S. & Sonesson, J. 2014. STIG-projektet 2010–2014. Report 818–2014. Skogforsk. (In Swedish with English summary)
- Friberg, G. Bergkvist, I 2016. The effect of working practices and DTW-maps on driving damage in forestry. Report 904–2016. Skogforsk. Uppsala. (In Swedish)
- Flisberg, P., Forsberg, M. & Rönnkvist, M. 2007. Optimization based planning tools for routing of forwarders at harvest areas. Canadian Journal of forest research 37(11), 2153–2163.
- Jönsson, P., Westlund, K., Flisberg, P. & Rönnqvist, M. 2011. Forwarder planning of timber, pulpwood, forest energy and stumps. Report 753. Skogforsk (in Swedish).
- Lundgren, J., Rönnqvist, M. & Värbrand, P 2010. Optimization. ISBN: 9789144053080. Förlag: Studentlitteratur AB.
- Willén, E., Andersson, G. (2015). Operational planning - A comparison of seven forest companies (in Swedish). Uppsala, Sweden, Skogforsk.

4. Main extraction routes planning - application Ajourakone

Introduction

Ajourakone is a web-based application for positioning and visualization of main extraction roads for thinning and final felling sites. The functional aim of the Ajourakone application is to calculate and visualize the locations of main extraction roads in thinning and final felling stand so that the extraction roads are in optimum locations on the basis terrain model and variables derived from that. Main extraction road location information can be used in planning of cutting and during the cutting operations.

The first field testing period of Ajourakone took place in Autumn 2017. The second testing period started at the end of December 2017 and continued until the end of April 2018. The second testing period was longer and all Metsäteho's shareholder companies participated. Forest machine manufacturers and LUKE's persons, participating the Efforte project, were also invited to test the application. Ajourakone has been programmed by CGI under a supervision of Metsäteho and Metsäteho's shareholders. The background for the application can be found from Järvinen's (2017) diploma thesis.

Functional Principle of Ajourakone

In order to find suitable routes from the terrain, some sort of road network must be created on the terrain for which the optimized routing is generated according to certain principles. Ajourakone generates a routing network on the map, where hexagonal is the basic structure (Figure 10). Points at their corners are called nodes and lines connecting the nodes as arc. There are also nodes in the center of the hexagons, which are connected to the other nodes with arcs.

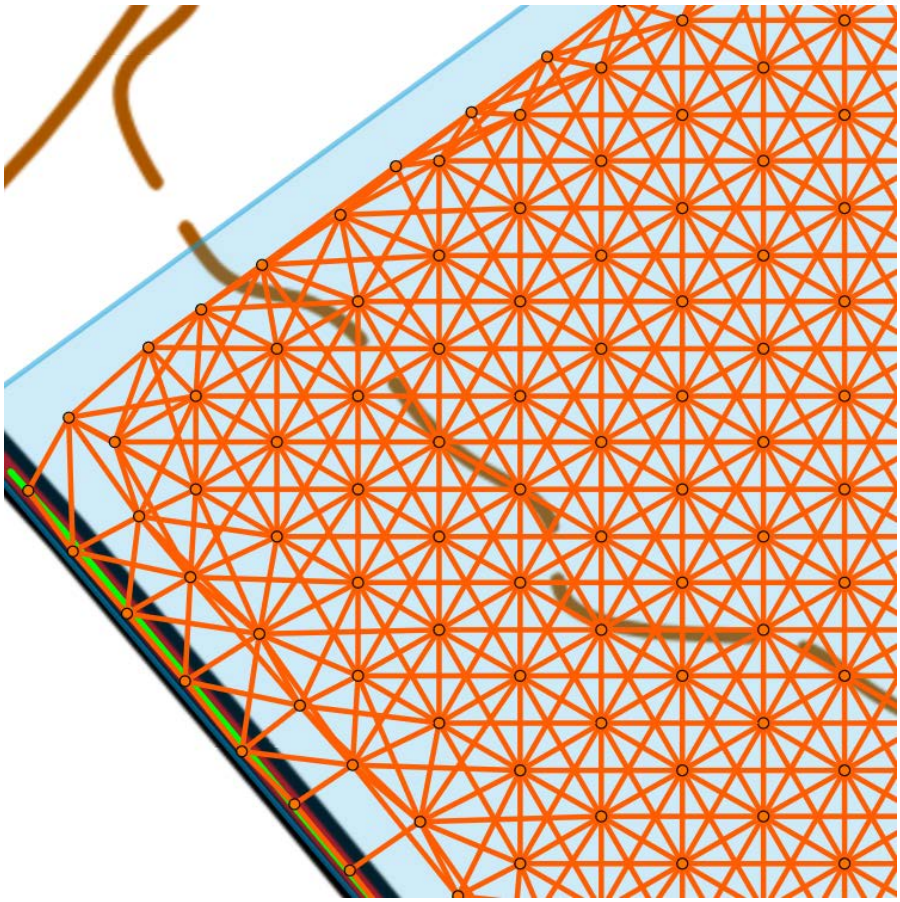

Figure 10. A routing network is created for the harvesting site. The basic structure is hexagon consisting of nodes and arches.

The calculation of optimal paths is based on the values of the arches. The value of each arch is based on the terrain form, the moisture index and the values of terrain trafficability map. Additionally, if an editable element hits an arc, like for example ditch, it affects the arc value. For example, if the arch is in a prohibited area or crosses a road that cannot be crossed, the value of the arch is so high that it will probably not be selected as a route in outcome. In the optimization result, the lowest total cost will form the extraction routes (Figure 11) to certain points on the harvesting site when starting from the landing and taking into account the set distance between the extraction routes.

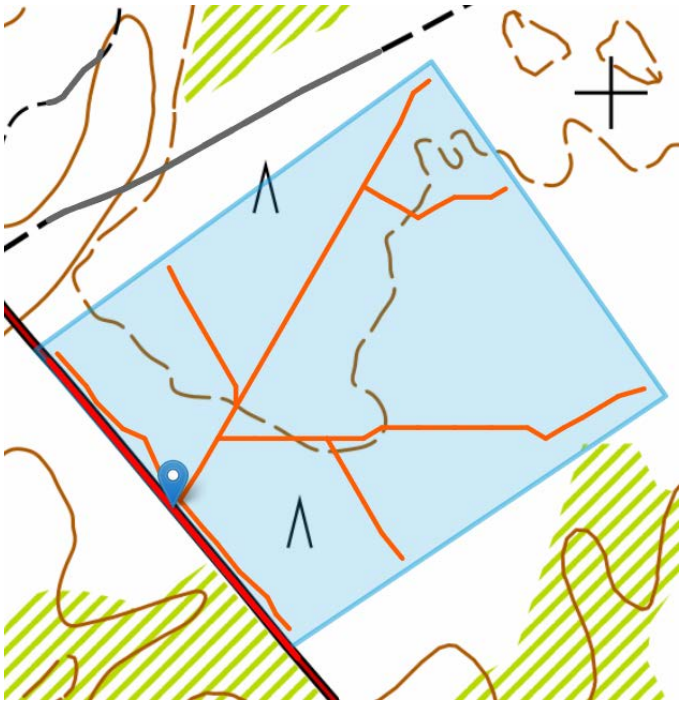

Figure 11. Landing along the road side and the main extraction roads on the harvesting site.

User can adjust the distance between the extraction roads, the bearing capacity (moisture level), and the limit values of inclination. Tree stock data is not yet utilized.

Results of test periods

The first testing period of Ajourakone took place in Autumn 2017. The application was tested in the field by the harvesting supervisors of Metsä Group, Stora Enso, UPM and Metsähallitus. The main outcome of the testing period was that the application must include a tool package to give more information of no-go areas and recommended routes. Therefore, a technical tool package was added to the application to enable:

- bordering of areas out of harvesting (no-go areas),
- defining routes/paths that must be used. Prevent use of certain roads or passing of certain ditches.
- multiple landings and
- improvement of moisture index visualization and the use of oblique hill shading when marking of harvesting area.

It is possible to adjust extraction road spacing in Ajourakone, i.e., the distance between extraction routes. The higher the value of spacing parameter is, the higher the distance between different extraction roads is. On the other hand, if the parameter value is low, the density of the extraction road network is high and the user might not perceive some strip roads as extraction roads. This confused some users.

The second testing period of Ajourakone was launched at the end of 2017. The aim of this period was to implement the extraction road plan in practice. The staff members of the companies had to thoroughly familiarize themselves with the application characteristics and to make a feasible extraction route plan for the harvesting area. The extraction route plan was given to the harvester operators and they tried to implement it. The routes driven by forwarder were recorded. Harvesting area could be first thinning or final felling.

The number of returned feedback harvesting areas was less than ten. Harvesting companies have had a busy spring because of the good harvesting circumstances. Nevertheless, based on the feedback from the testing period, it was found that the microstructure of the terrain has higher effect on the direction of the extraction routes as expected. For example, the various deep ditches in the same area affect the design of the extraction routes. Therefore, the application was developed to take better account the micro elements of the terrain in total. It was also noted that the Ajourakone avoided a little too much incline, so the influence of inclination was adjusted. In addition, picking of values from background material layers was fine-tuned.

Discussion

At this phase of development of Ajourakone, the application is at its best in large and challenging harvesting sites when multiple route options are available. In addition, sites with varying altitudes in terrain, including low bearing points, are suitable for the Ajourakone. In Finland, the average harvesting site size is 1.5 ha. On small sites the number of route options is small and therefore the need for design is not so high.

On the other hand, with flat and well-bearing sites that can be driven anywhere in principle, the design need is also low and the most important thing to design is a minimal strip road network. With this type of site, the strip road network produced by the Ajourakone with this calculation algorithm may not be optimal from the driving distance point of view.

Plans for validation

The number of feedbacks in spring feedback collection was low and many companies reported that they could test the application during the summer. Hence, feedback will be continued until the end of September 2018. So far the Ajourakone also lacks of tree data and that will be included into the background data and calculation procedure next.

References

Järvinen, T. 2017. Paikkatiedon hyödyntäminen koneellisen puunkorjuun ajourien suunnittelussa. [ENG: Geographic information in mechanical logging optimization] Diploma thesis. Geoinformatics, Aalto University. 44 p. (In Finnish)

5. Forest machine data for modelling soil bearing capacity

Introduction

Modern forest machines with hydrostatic transmission and CAN-bus engine and transmission management can be used to measure power expended in travelling. At constant speed on level ground the power is expended in overcoming motion resistance, which in turn is directly related to wheel sinkage and hence vehicle mobility or site trafficability. The harvester always precedes the heavier forwarder on the site, making it feasible to use it to collect data on site trafficability to produce a mobility map for the forwarder. The process can be fully automated and comprehensive data collected at low cost.

The most accurate method for determining the power expended in machine travel on the basis of CAN bus data is directly measuring the effective hydraulic pressure and flow rate of the transmission. An alternative way of is the indirect method of using engine output determined on the basis of torque and engine speed read from CAN-bus. Since not all engine power is converted into hydraulic power the efficiency of the engine-hydraulic transmission system has to be determined.

Based on field studies in 2016 and 2017, Luke has also developed a methodology that detects and interprets soil bearing capacity based on the relationship between engine power and travelling speed, corrected by terrain slope angle. The interpretation is executed via recording of data communication in CAN bus network of a forest machine. The studies also aimed at finding out the effect of brush mat and bogie tracks in the CAN-bus measuring principle. Bogie tracks increase the inherent motion resistance of the harvester and the measuring system should be sensitive enough to detect this, if it is to be used in practice.

Material and methods

2016 studies in Vihti in Southern Finland

CAN-bus trafficability mapping was tested with an 8-wheeled Ponsse Scorpion King harvester and 8-wheeled Ponsse Elk forwarder equipped for collecting transmission power expenditure in addition to appropriate standard CAN-bus information. Trafficability was also mapped based solely on diesel engine power in order to eliminate the need for an extra pressure transducer needed for transmission power monitoring.

The CAN measurement principle was first tested on an even forest road with gravel surface and an even collector trail with good bearing capacity to obtain reference values for rolling resistance in conditions of low average rolling resistance and low level of variation.

For trials in operational forest environment a 1,1 km test track was laid out. The route passed through various soil types: clay, sandy till, and bedrock partly covered by 5 to 15 cm layer of fine-grained mineral soil and organic material. The terrain profile varied from flat to slightly undulating, and significant soil moisture variations occurred along the route. Along the test track nine 20 m long test sites were selected. In order to rule out the influencing

factors outside rolling resistance and specially to determine the accuracy of the indirect measurement principle the test sites were designed as straight as possible to avoid the effect of turning resistance on motion resistance. The direct measuring principle was applied on forest road and collector trail and on four test sites. The indirect measurement principle was used on all test sites.

The test track was first opened up by an 8-wheeled Ponsse Scorpion King harvester with a mass of 22 500 kg. The harvester was equipped with wheel chains on the rear wheels on front and rear bogies. Thereafter a loaded 8-wheeled Ponsse Elk forwarder with a mass of 30 000 kg passed the route 2 to 4 times. The forwarder was equipped with wheel chain on the rear wheels of the front bogie and Olofsfors Eco Tracks on the rear bogie. Both machines were equipped with Nokian Forest King F2 710/45-26,5 tires.

On the test sites, penetration resistance was measured after the harvester pass with Eijkelkamp penetrologger electronically recording penetrometer between wheel ruts at one-meter intervals. Two to four 60 mm diameter mineral soil samples per test site were taken for grain size analysis. Rut depths were manually measured after each pass at one-meter intervals using a horizontal hurdle and a measuring rod. Rut depths were measured after each vehicle pass. Test site 2 was covered with logging residue to find out the effect of brash mat. Accurate GPS coordinates of the start and end points of the test sites were recorded.

2017 studies in Kuru in Central Finland

The field study arrangements in 2017 were in principal similar to those of 2016. In 2017 one of the aims was to find out the effect of bogie tracks in the CAN-bus measuring principle. The test trial in the forest therefore comprised two parallel test trails, one driven with and the other without bogie tracks. Soil conditions ranged from peatland to mineral soil. Both trails included five test 20 m long test blocks, each having four 5m long study plots. The aim was to get results on more coarse-grained soils with variation in moisture content. Measurement of soil properties and rut depth was similar to 2016 experiment with the addition of laboratory and in-situ measurement of soil moisture. Also, the wheeling test protocol was similar.

The study trails were first harvested with 8-wheeled Ponsse Scorpion King harvester similar to that of the 2016 field trials. On trail one, the wheels in the front bogie were equipped with chains and rear bogie with Olofsfors Eco Tracks. On trail two, the wheels in the front bogie were equipped with chains and rear bogie had bare wheels. The fundamental difference in harvester rolling resistance with and without bogie tracks was studied on a level forest road. After harvesting the extraction trails were passed with a loaded 8-wheeled Timberjack 1210E forwarder with a mass of 32000 kg. Both wheels in the front bogie were equipped with chains and the rear bogie with tracks.

Rolling resistance calculus

Diesel engine power was determined on the basis of engine control unit calculated torque and engine speed read from CAN bus. CAN bus data was read from Ponsse Opti control system and hydraulic pressure transducer data was recorded with a datalogger supplied by Creanex Ltd. The engine output to transmission hydraulic power conversion degree of efficiency was determined by simultaneous direct and indirect measurements on a collector trail (2016 studies) or a gravel road (2017 studies). A linear model was fit to the data and used to convert engine power into transmission power on the test sites. Transmission hydraulic power was calculated using an equation supplied by Ponsse Plc, having differential pressure over hydraulic pump, pump and motor volume per one rotation, hydraulic unit rotational speed and hydraulic efficiency as variables.

The harvester hydraulic transmission is followed by a conventional mechanical transmission with a drop box, final drives front and rear, gears inside the bogies and wheel hub reduction. The sum of gear meshes with an assumed coefficient of efficiency of 0,97 was 10 resulting in a total efficiency of 0,74. Transmission hydraulic power was multiplied by mechanical transmission efficiency to obtain power on wheels.

For calculating slope force, slope angle in the direction of travel was determined on the basis of 2m by 2m digital terrain model having a vertical accuracy of 0,3 m and the GPS path recorded during the test drives.

During normal work in easy terrain conditions of the test sections both harvester and forwarder normally travel at a near-constant speed. The harvester stopped for cutting on the test sections and then moved to the next work station. Acceleration of the machinery was dealt with by selecting a near-constant speed subset of data from the speed range 0,5 to 1,0 ms-1. Given the considerable mass of the harvester, accelerations and decelerations on the near constant speed range were minor and assumed here to cancel out each other.

The test sections were laid out as straight as possible. The effect of turning resistance and the power expended by articulated steering were therefore omitted. The effect of obstacle resistance was omitted as well. The cooling of the hydraulic system of a modern full-size harvester is a big power consumer and it was assured, that the cooling fan was not on during the tests drives.

Machine GPS data was used for determination of vehicle speed needed for converting expended power into resisting force. Mismatch in timestamps of CAN bus and GPS data, and that acquired by additional datalogger, was accounted for by determining a constant lagtime maximizing correlation of the datasources.

Results

2016 studies

According to particle size analysis results the test site mineral soil can be classified into even-graded soils and tills (Fig. 12). Test site 6 was fine sand and site 9 medium sand. Sites 1, 2, and 5 were silty sand till, sites 3 and 8 sandy silty clay till and sites 4 and 7 silty clay till.

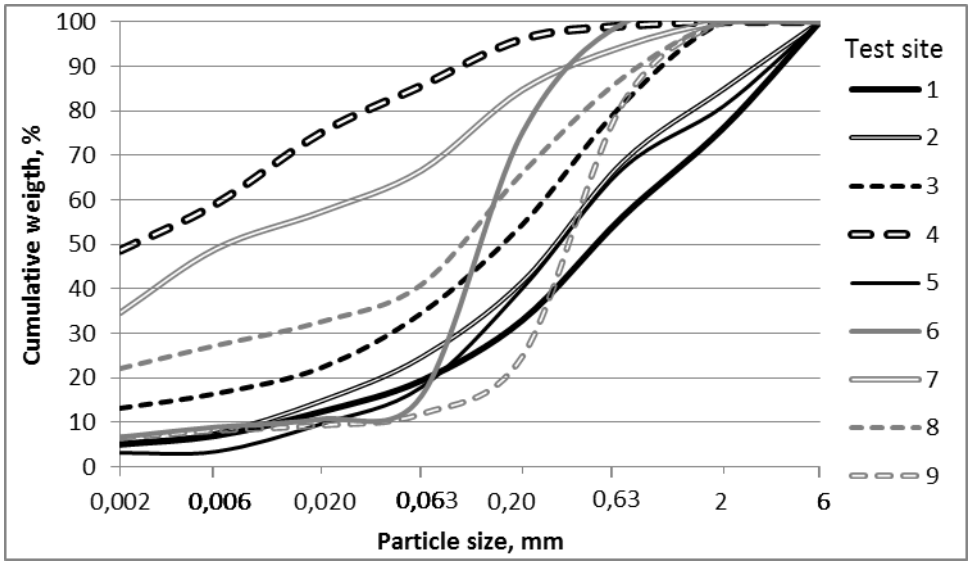

Figure 12. Soil grain size distribution on the test sites.

Average penetration resistances down to average penetration depth on the test sites are shown in Figure 13. The sites can be divided into two groups: the penetration resistance of the wet sites 3,6,8 and 9 on the surface layer down to 35 cm is well below that of the dry sites. Sites 1, 2 and 5 located on bedrock have shallow penetration depth with penetration resistance rising rapidly upon meeting the bedrock surface. The penetration resistance of site 2 does not describe its high bearing capacity as the shallow layer of soil on top of the bedrock was fairly loose and the bearing capacity of bedrock does not show in the measurement result. Clayey sites 4 and 7 have a hard-dry core layer. Average penetration resistance 0 to 20 cm on top of the mineral soil layer is presented in Figure 14. Variation especially in average top soil penetration resistance was pronounced.

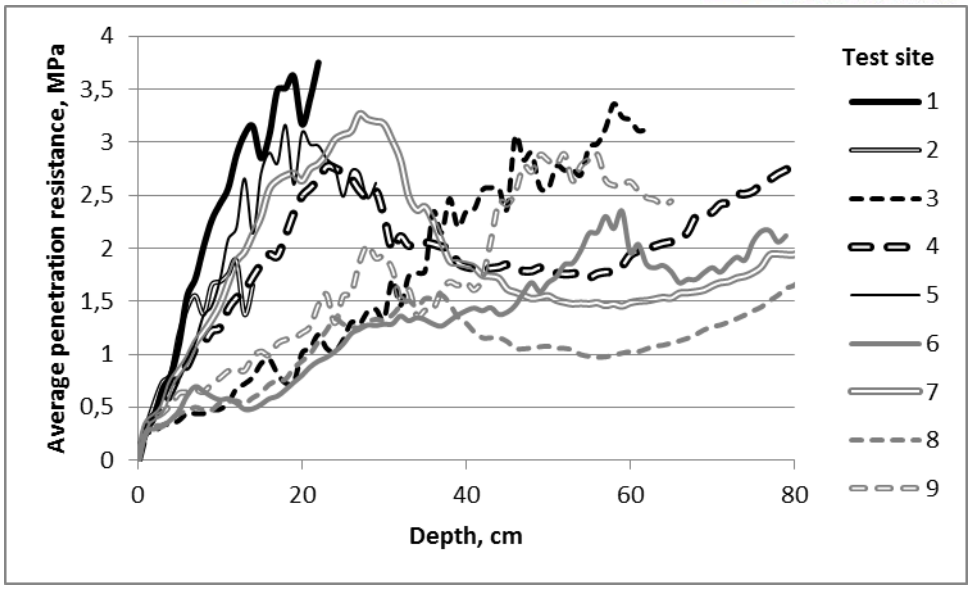

Figure 13. Average penetration resistances down to average penetration depth per the test site.

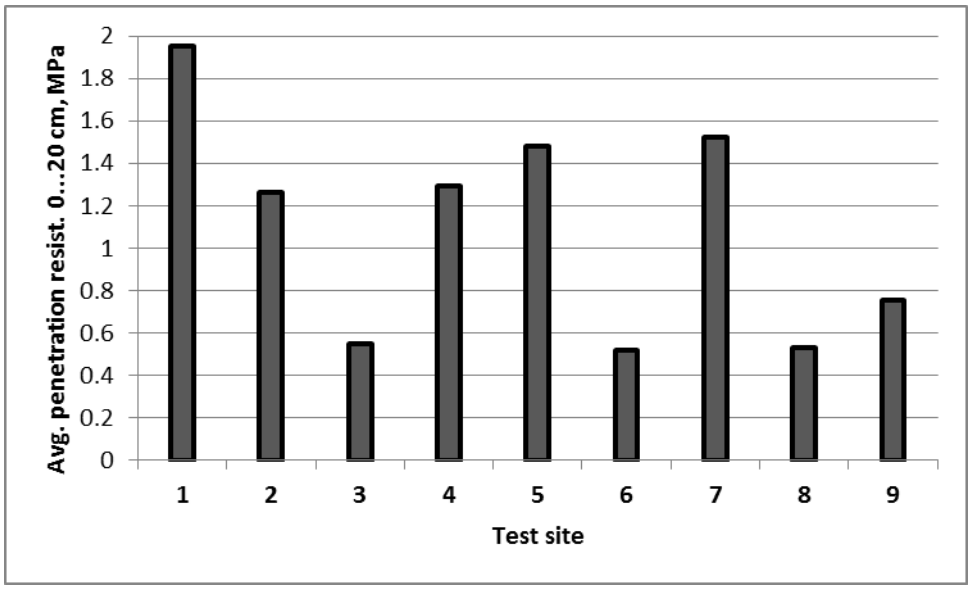

Figure 14. Average penetration resistances 0 to 20 cm on the test sites.

Direct and indirect measurement methods of power expenditure were then compared in harvester rolling resistance coefficient calculus on occasions where both methods were applied (Fig. 15). The accuracy of indirect measurement was adequate for performing the rest of the test drives.

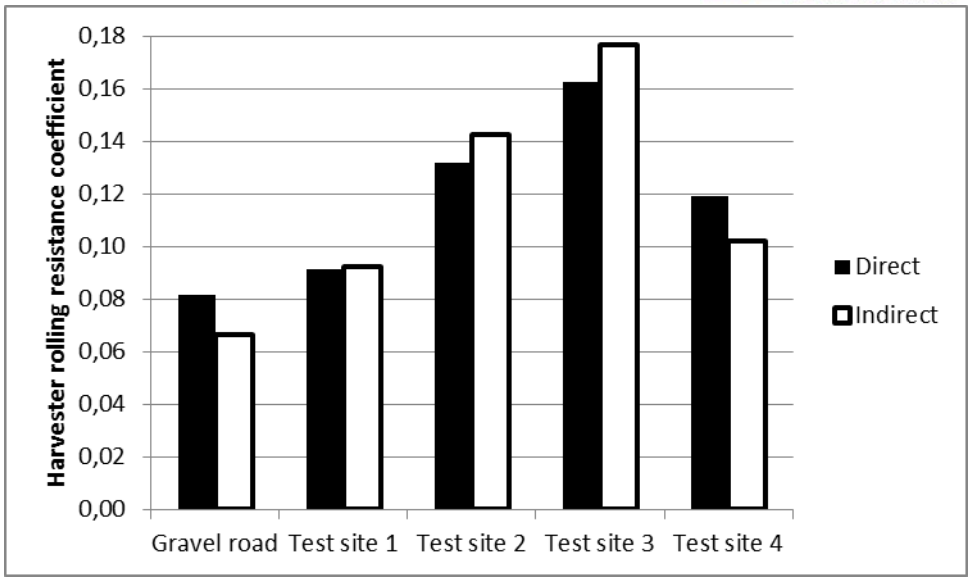

Figure 15. Directly vs. indirectly measured rolling resistance coefficient results.

Averages harvester rolling resistance coefficients and rut depths for harvester and forwarder per test site and vehicle pass are presented in Figure 16. The highest harvester rolling resistance values were measured on the softest test sites 3, 6 and 8, which is in accordance with the highest harvester and forwarder rut depths measured on the same sites. The effect of low soil strength of the sites 3, 6 and 8 can be seen in rut depths and maximum number of forwarder passes. The soil strength of site 9 would have permitted further passes but the entrance to the site was through site 8 which was no longer trafficable. The rolling resistance coefficient on site 9 thus describes its trafficability well despite of low number of passes.

Low values of harvester rolling resistance should be expected on sites with shallow soil layer on top of bedrock and good bearing capacity. This was the case especially on site 1. According to the penetration resistance measurements on site 2, the soil on top of the bedrock was weaker, but the depth to bedrock was shallower. Thus, the main reason for higher rolling resistance was probably the brash mat, which also partly contributed to the rut depths lower than on site 1. Site 5 also had high soil strength and low rut depth, but the obstacle resistance caused by the considerable surface roughness may have increased the measured rolling resistance coefficient.

Rolling resistance measurements on the clayey sites 4 and 7 were somewhat inconclusive. Rolling resistance particularly on site 7 is higher than could be expected based on high penetration resistance and low rut depth. On the basis of soil strength and rut depth, the rolling resistance coefficient on site 7 should be lower than that on site 4. The rolling resistance on site 7 is high also in comparison with site 9, having clearly weaker soil and deeper ruts.

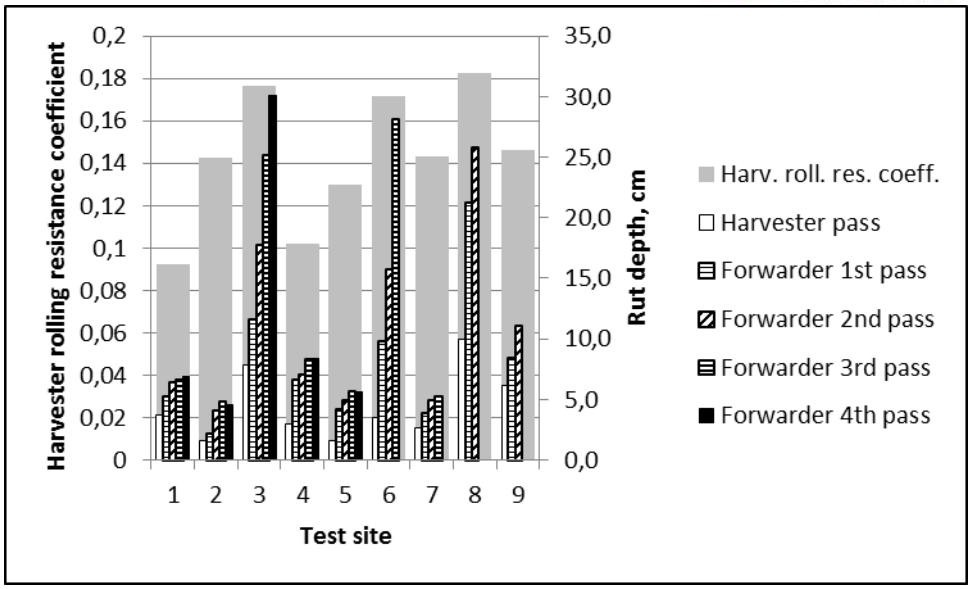

Figure 16. Harvester indirectly measured rolling resistance coefficients compared to rut depths for harvester and forwarder. All values are averages per test site and vehicle pass.

2017 studies

Soil moisture content and average mineral soil penetration resistance 0 to 20 cm on mineral soil tracks are presented in Figure 17. Tracks 1 and 2 were laid on peat soil. Mineral soil track 4 had the highest strength and lowest moisture. Track 6 was covered with a organic soil layer of 20 to 30 cm and it had high moisture content. The soil type on mineral soil tracks 3 to 6 was silty fine sand ant the variation between tracks was small (Fig 18).

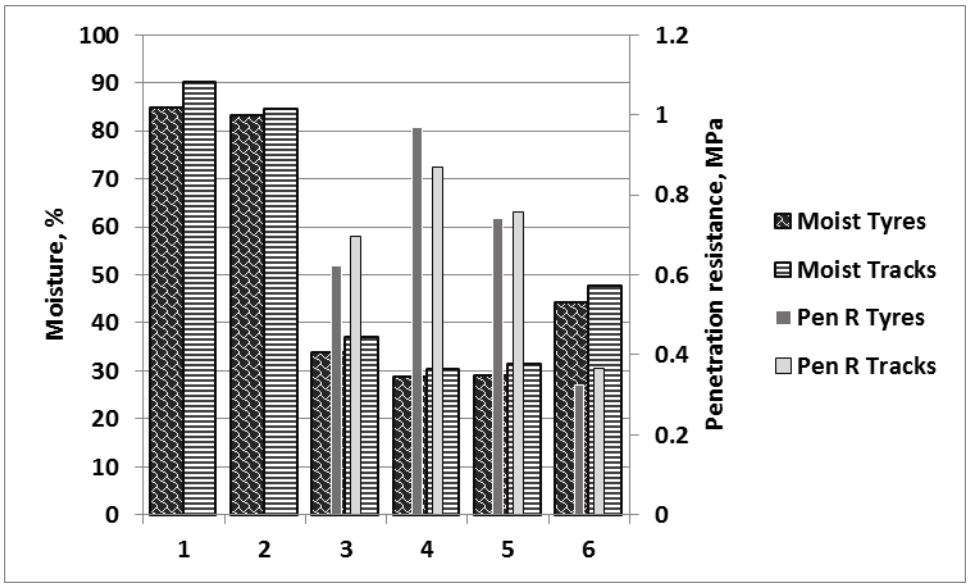

Figure 17. Moisture content and penetration resistance 0 to 20 cm on test tracks. 'Tracks' and 'Tyres' refer to harvester equipment.

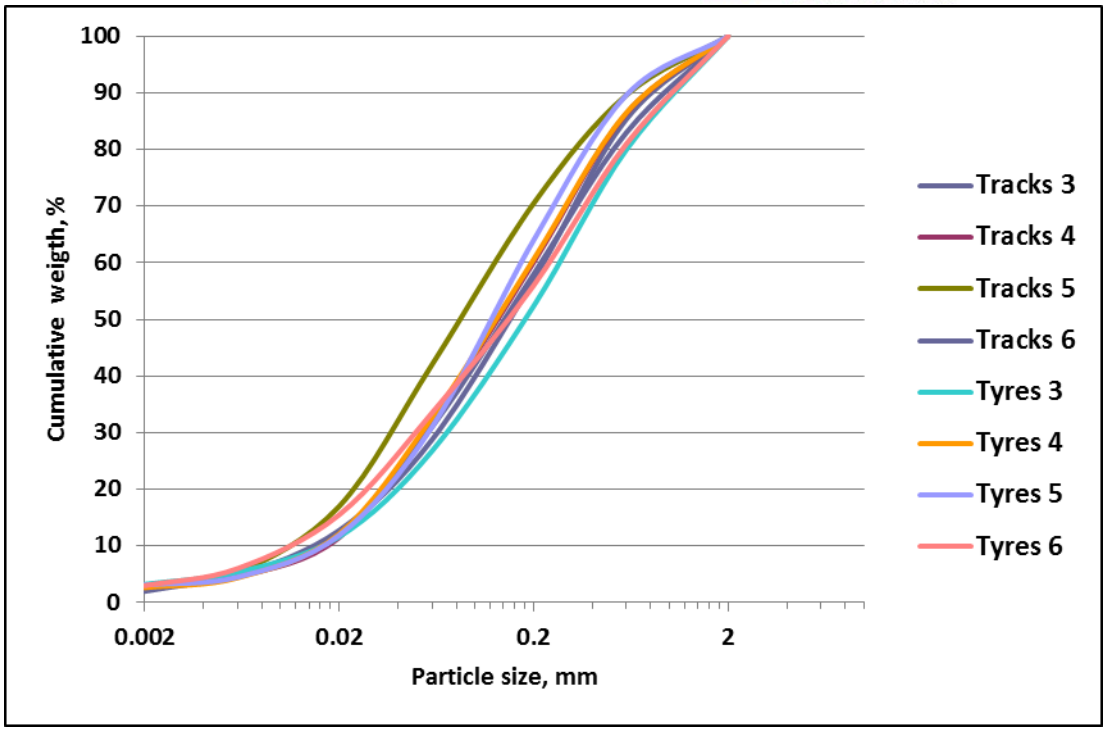

Figure 18. Grain size distribution of the mineral soil tracks. 'Tracks' and 'Tyres' refer to harvester equipment.

Harvester motion resistance coefficients on the test sites are given in Figure 19. The increase in motion resistance on gravel road due to one pair of steel tracks was roughly 50% or 0,026 in terms of motion resistance coefficient. The increase due to steel tracks was assumed to be due to internal friction and it was subtracted from tracked test drive results in order obtain motion resistance toe to terrain (Fig 20).

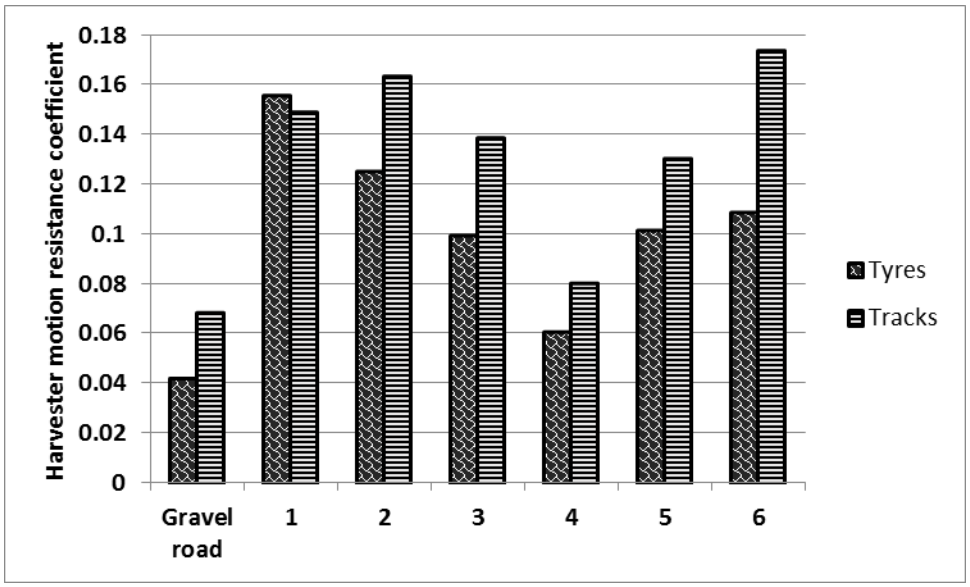

Figure 19. Harvester motion resistance coefficients on the test sites.

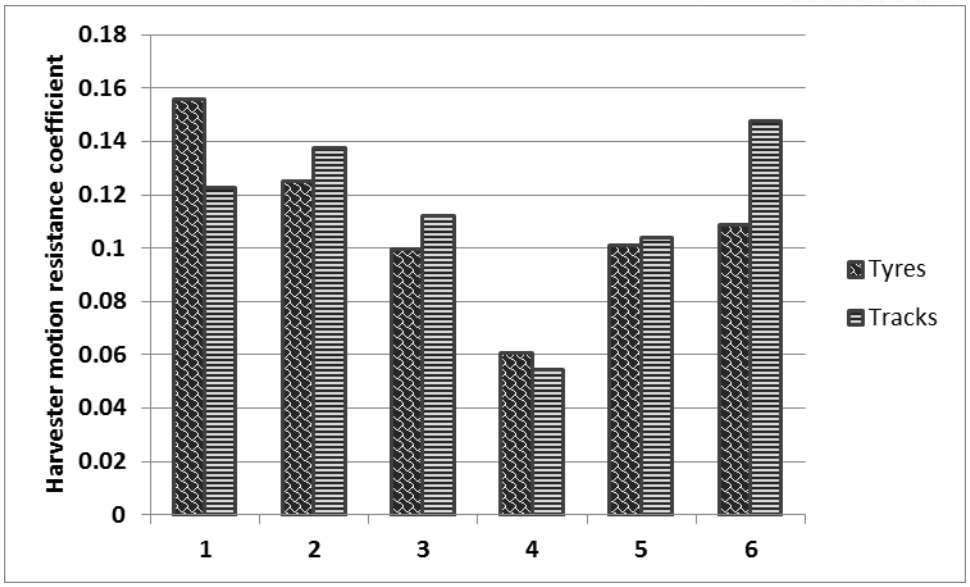

Figure 20. Harvester motion resistance coefficients on the test tracks due to terrain.

The bearing capacity of peatland tracks 1 and 2 was judged insufficient for forwarder travel. Rut depths on the first and second forwarder pass together with harvester motion resistance coefficients are presented in Figure 21. The mineral soil track 4 with the best mobility conditions is clearly distinguishable both in terms of harvester motion resistance and forwarder rut depth, as is also track 6 with the worst conditions.

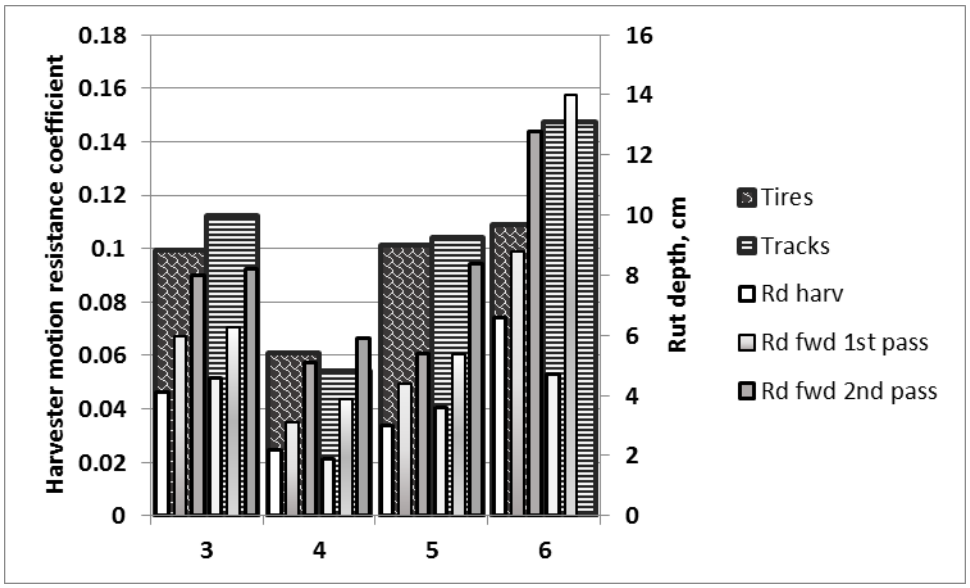

Figure 21. Harvester motion resistance coefficient and forwarder rut depth on first and second pass for sites 3 to 6..

Track 6 was judged not trafficable for further forwarder passes. The remaining mineral soil tracks 3 to 5 were passed five times with a loaded forwarder (Fig. 22). Again here the strongest and driest track 4 clearly stands out from the softer and moister tracks.

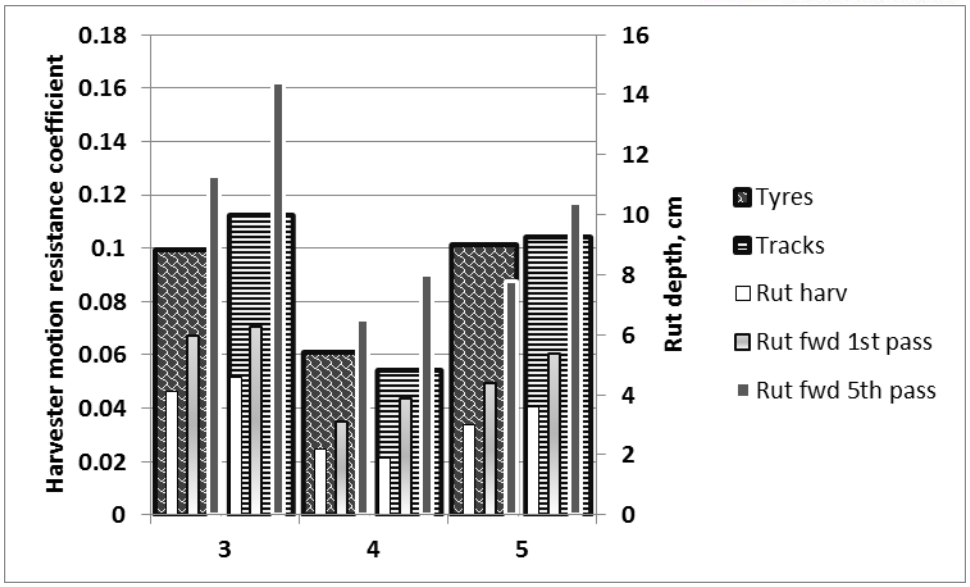

Figure 22. Harvester motion resistance coefficient and forwarder rut depth on first and fifth pass for sites 3 to 5.

Discussion

Assessing forest harvester rolling resistance by CAN-bus data is an interesting possibility to map harvesting site trafficability by actually measuring mobility variables. Not only is this a huge step forward compared to prevailing human estimation of trafficability, but it is also very cost-effective and comprehensive. As modern harvesters are practically ready for indirect power recording the extra cost of trafficability mapping is negligible. Employing the system in all new harvesters would result in a rapid build-up of the database on harvesting conditions. This would support new static and dynamic bearing capacity and moisture prediction models prepared for operational use. Besides serving as input for optimization of timber transport to the landing site, the map on trafficability would also support to decision making on forwarding scheduling, machine size and equipment.

The experiments were performed on relatively flat ground. In steeper downhills the role of hydraulic pump and hydraulic motor is inversed: the hydraulic transmission is used for slowing down the machine as the diesel engine is braking the machine. The applied equation of hydraulic transmission power is not tested in these conditions. As soil strength also affects tractive force, the variable most suited for trafficability mapping would be net traction coefficient. Harvester wheel slip in frequent stop-and-go cycles, characteristic for timber cutting with a harvester, could possibly be used to determine it.

The accuracy of indirect measurement was estimated promising especially for practical big data applications where the amount of data collected is large. The sites with the poorest bearing capacity were detected best, but also mineral sites with slightly differing properties were distinguished. Also, sites with good trafficability were easily pointed out. The use of steel track did not compromise the measuring principle.

Plan for validation

Due to laborious field work, the data of this study was fairly small. It is therefore difficult to decide if some discrepancies in results are due to unexplained phenomena or the limited accuracy of the method. The harvester engine management or transmission systems were not originally designed for trafficability measurements, let alone scientific ones. Less intensive field trials in co-operation with Ponsse Plc are therefore planned for the autumn 2018. The aim is to include the indirect measuring system into the harvester by the manufacturer so, that all data collection would be automated. The resulting rut depth would then be controlled manually. The work would be done on normal harvesting sites, which would be selected with the help of soil moisture maps. Rut depth after forwarding would also be controlled in worst scenario cases.

6. Automatic post-harvest quality assessment

Introduction

Off-road traffic of heavy forest machines can cause soil damages. Compaction and rut formation of soil have harmful impacts on economy and ecology. Rutting is regulated by forest laws and forest certification standards. Continuous rut depth monitoring could be a method to control and improve post-harvest quality. Continuous rut depth monitoring can be carried put multiple methods, like photogrammetric or Light Detection and Ranging (LiDAR) methods. Photogrammetric methods are sensible for light conditions. LiDAR, as an active sensor, can be utilized at various conditions.

We tested 2D-LiDAR sensor for continuous rut depth monitoring in two field experiments in Vihti in Southern Finland and in Kuru in Central Finland.

Material and methods

2016 studies in Vihti in Southern Finland

Field studies were carried out in 2016 in Vihti Southern Finland (60°24'N, 24º23'E in WGS84), with same test trail and machines described in chapter 4, but with total length of 1,3 km and 11 study plots.

Light Detection and Ranging (LiDAR) sensor (SICK LMS-511) was mounted in the back of the forest machines at a 45-degree angle (Figure 23). The LiDAR sensor measured in 25 Hz frequency the distance and the angle to target ranging over 190 degrees with an angular resolution of 0.1667 degrees. Mounting the sensor at a 45-degree angle enabled the measurement of both the position and the speed independently from the forest machine's Global Positioning System (GPS). The rut depths were manually measured at 1-m intervals from both ruts (n ~ 40) after each vehicle pass (n = 3. . .5) using a horizontal hurdle and a measuring rod to provide reference for the LiDAR-derived rut depths.

The LiDAR-derived point cloud data were processed with specially designed software developed by Argone Ltd to produce raw rut depth data with x- and y-coordinates. Position and speed were calculated by recognizing the trees on both sides of the track from the point cloud data (Figure 23). The output data included momentary position, vehicle speed and the maximum rut depth for ruts. Data for comparing LiDAR and manual rut depth measurements were picked from the raw rut depth data by taking an average of the raw rut depths located at ± 25 cm distance from the manual measurement spot.

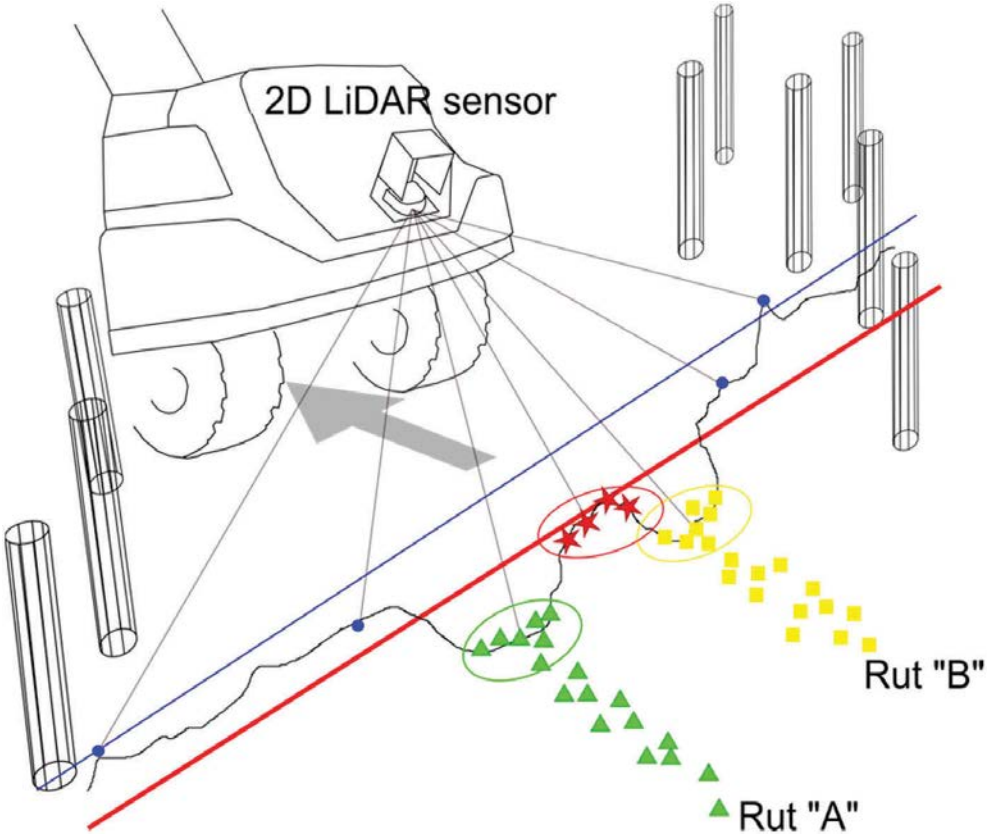

Figure 23. Point cloud analysis and rut detection. Preliminary terrain level (thin blue line) is adjusted according to the terrain level found between the wheels (thick red line). Ruts were located and tracked with the Monte Carlo localization method. Circles (from left to right) indicate the points located in rut "A" (in green triangles), the points located between the ruts (in red stars) and the points located in rut "B" (in yellow squares). Temporary tree map (vertical cylinders) enables tracking the distance traveled.

2017 studies in Kuru in Central Finland

Field studies were carried out in 2017 in Kuru, Central Finland (61°56'N, 23º50'E in WGS84) with same plots and machines described in chapter 4. Same LiDAR-sensor was utilized than in previous experiment in Vihti. LiDAR-sensor, laptop computer with software developed by Argone Ltd and GPS/Glonass- receiver were installed to be a standalone system. The LiDAR-sensor was mounted directly downwards. GPS/Glonass was used to positioning.

Software was developed to realize real-time rut depth monitoring. Fixed angles of rut bottoms and reference terrain were set preliminary in scanning sector of LiDAR sensor (Figure 24). Lowest 2 percent of LiDAR observation points were included in each determination of rut bottoms and reference levels to reduce noise of scanning. Rut depth was calculated as a remainder of rut bottoms and neighboring reference levels. Due to inaccuracy of GPS/Glonass system was LiDAR data localized to plots with timestamps of plot signals.

Rut depths were manually measured with levelling laser from both ruts on three lines per plot after every machine pass. Reference level for every sample point was measured prior to

test drives. To take compaction of moss layer in manual measurement into account were 5 cm reduction made of LiDAR results.

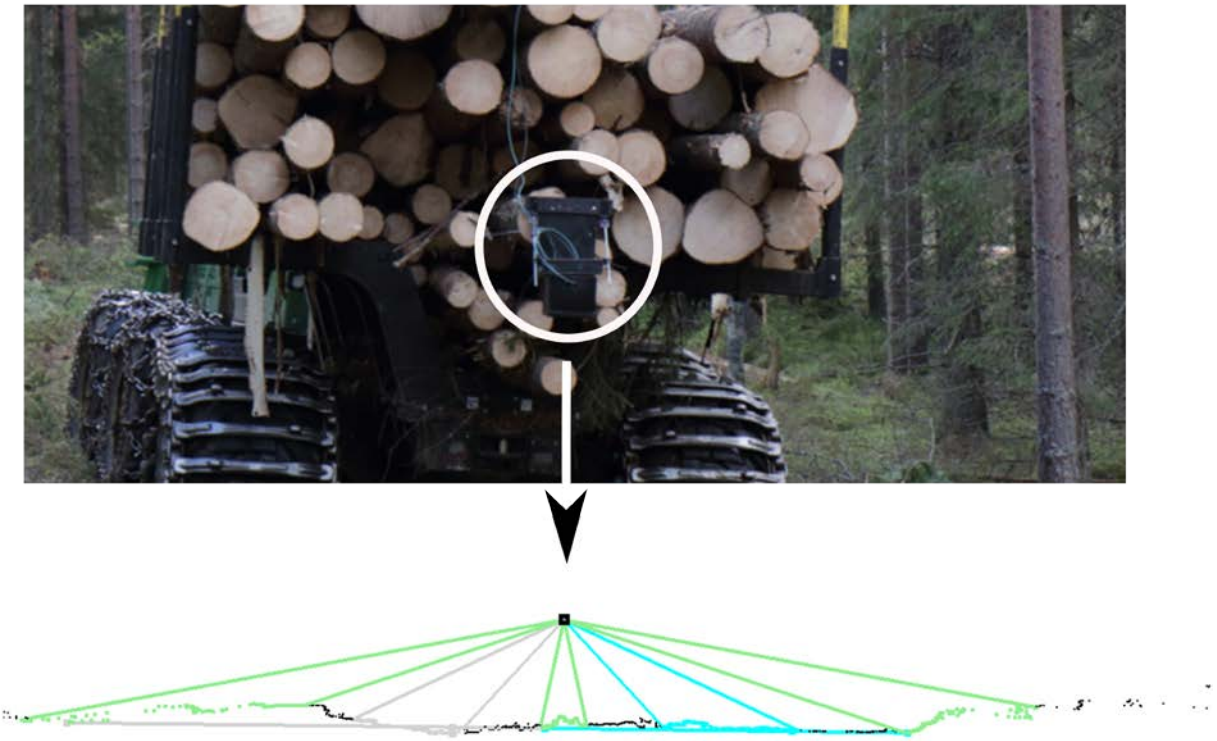

Figure 24. 2D-LiDAR sensor was mounted in the back of forwarder. The view of software window demonstrates LiDAR sensor (black square), LiDAR observations (dots), rut bottom angles (grey and blue lines) and reference terrain level angles (green lines).

Results

2016 studies in Vihti in Southern Finland

The results in regard to rut depth measurements with the laser device were promising, whereas detecting forward speed on the basis of laser data proved unreliable. The descriptive statistics together with the soil information from soil map and soil samples taken during the field campaign are shown in Table 1. While the overall RMSE across the test sites and vehicle passes was 3.49 (cm), it is clear that in certain test sites (T2, T3, T10) the errors were higher than in others. Considering the ruts in rough classes of 0-10, 10-20 and above 20cm, we got 5 cases out of 42 where the laser classifies the ruts differently (highlighted with light red and light blue in Table 1).

Table 1. Descriptive statistics of manually and laser-derived rut depths per test sites with information on the soil. Differences in laser and manual classification highlighted in red and blue.

Test site	Descriptive statistics	MANUAL	LASER

soil type		1st pass	2nd pass	3rd pass	4th pass	5th pass	1st pass	2nd pass	3rd pass	4th pass	5th pass
T1	mean n=38 per each pass	3.7	5.2	6.4	6.7	6.9	4.1	5.3	5.5	6.8	6.2
bedrock	std	4.5	4.5	4.7	4.0	4.4	4.7	6.6	6.7	5.9	6.7
fine sand moraine	RMSE (n~38)						6.23	8.35	7.58	6.68	6.7
	dif in means						0.38	0.13	0.94	0.10	0.72
	dif as % from manual mean						10	3	15	1	10
	dif as % from manual std						8	3	20	3	16
T2 *logging residues:	mean n=40 per each pass	1.9	2.1	4.1	4.8	4.6	4.7	8.8	7.0	8.3	7.7
bedrock /	std	4.5	6.4	5.5	5.4	5.8	10.8	8.6	9.4	9.3	8.1
coarse sand moraine	RMSE (n~40)						11.37	13.46	10.27	12.76	9.56
fine sand moraine	dif in means						2.83	6.70	2.89	3.55	3.08
	dif as from manual mean						149	319	70	74	67
	dif as from manual std						63	105	53	66	53
	*exceptions	n=38					n=38				
T3	mean n=40 per each pass	7.9	11.6	17.8	25.2	30.1	4.9	4.0	16.5	17.8	25.5
bedrock/	std	6.4	7.8	12.6	14.9	15.6	8.8	10.3	16.9	16.2	20.4
clayish coarse sand	RMSE (n~40)						10.13	16.10	22.39	26.23	14.76
clayish fine sand	dif in means						2.97	7.60	1.22	7.33	4.53
	dif as from manual mean						38	66	7	29	15
	dif as from manual std						46	97	10	49	29
T4	mean n=42 per each pass	3.0	6.6	7.1	8.3	8.4	5.0	5.9	5.8	7.2	8.7
silty clay /	std	2.1	2.7	2.7	2.9	2.7	6.5	7.5	7.5	7.4	7.7
clay	RMSE (n~40)						6.51	7.29	7.11	7.35	6.76
	dif in means						2.00	0.70	1.25	1.14	0.31
	dif as from manual mean						67	11	18	14	4
	dif as from manual std						95	26	46	39	11
	*exceptions					n=40					n=40
T5	mean n=40 per each pass	2.2	4.2	4.9	5.6	5.7	2.5	6.2	4.2	7.5	4.0
bedrock +	std	3.9	3.8	4.2	4.9	5.4	11.5	6.0	9.6	7.5	9.0
sand moraine /	RMSE (n~40)						12.42	8.11	11.05	9.20	10.89
fine sand moraine	dif in means						0.27	2.08	0.69	1.87	1.67
	dif as from manual mean						12	50	14	33	29
	dif as from manual std						7	55	16	38	31
	*exceptions	n=32					n=32				
T6	mean n=40 per each pass	3.6	9.8	15.7	28.1		1.2	7.5	10.4	25.4	
clay/	std	4.5	5.0	9.9	18.4		9.3	11.8	10.3	19.1	
sandy silt	RMSE (n~40)						11.83	12.53	13.10	23.02	
	dif in means						2.39	2.27	5.34	2.70	
	dif as from manual mean						66	23	34	10	
	dif as from manual std						53	45	54	15	
	*exceptions			n=38	n=36				n=38	n=36	

T8 clayish fine silt / clay	mean n=42 per each pass std RMSE (n~40) dif in means dif as from manual mean dif as from manual std *exceptions	2.7 2.5	3.8 2.9	5.0 2.6 n=40	5.3 2.9		10.0 16.9 18.73 7.26 269 290	3.9 6.4 7.55 0.02 1 1	3.7 5.9 6.22 1.52 30 58 n=40	6.9 7.4 7.72 1.61 30 56	
T9 clay / clayish coarse silt	mean n=42 per each pass std RMSE (n~40) dif in means dif as from manual mean dif as from manual std *exceptions	10.8 7.4 n=35	21.3 10.3	25.8 13.7			9.6 12.1 12.68 1.17 11 16 n=35	22.3 13.1 14.50 0.98 5 10	31.6 18.6 19.89 5.77 22 42		
T10 sand moraine/ fine sand	mean n=40 per each pass std RMSE (n~40) dif in means dif as from manual mean dif as from manual std *exceptions	5.5 5.7	8.5 6.6	11.0 8.9			9.6 14.6 17.67 4.10 75 72 n=34	14.9 18.8 20.48 6.45 76 98	19.1 14.2 15.71 8.12 74 91		
T11 clay / clayish medium silt	mean n=42 per each pass std RMSE (n~40) dif in means dif as from manual mean dif as from manual std *exceptions	2.6 2.3 n=32	3.4 2.7 n=36	4.3 2.8			0.9 3.1 4.55 1.68 65 73 n=32	3.7 4.8 5.80 0.34 10 13 n=36	3.9 4.8 4.51 0.36 8 13		
							RMSE per test site averages: 3.49				

The performance of the laser was further examined by fitting a linear model on the laser-derived rut depth data to explain the manually measured average rut depths for test sites. The linear model shows that the slope is close to 1 with statistically significant p-value, while the intercept's value of 0.32 is statistically insignificant, meaning that the intercept is not significantly different than zero (Table 2). Figure 25 shows the manual rut depths plotted against the laser-derived rut depths with the liner model depicted red line. The distribution of the points shows that there is no systematical over- or underestimation by the laser.

Table 2. Summary of linear model and linear mixed effect models for rut depth

	estimate	standard error	t-value	p-value	Additional info:
linear model: manual test site means ~laser-derived	(intercept): 0.32	(intercept): 0.89	(intercept): 0.36	(intercept): 0.72	adj. R2: 0.77

test site means n= 42	laser: 0.93	laser: 0.08	laser: 11.80	laser: 1.32e-14	res standard error: 3.54
mixed effect model: manual test site means ~laser-derived test site means, random ~1|test site n=42 groups:10	(intercept): 0.83 laser: 0.86 T1 intercept: 0.98 T2 intercept: -2.49 T3 intercept: 6.28 T4 intercept: 1.07 T5 intercept: 0.37 T6 intercept: 4.39 T8 intercept: -0.88 T9 intercept: 1.11 T10 intercept: -3.53 T11 intercept: 0.98	(intercept): 1.16 laser: 0.06	(intercept): 0.72 laser: 14.52	(intercept): 0.48 laser: 0.0000	within group res: med: 0.15 Random effects: StdDev: (Intercept): 3.06 Residual: 1.98

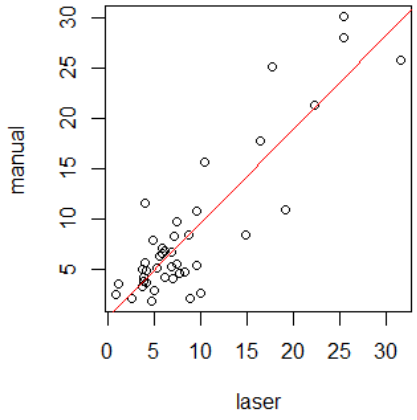

Figure 25. Manually measured rut depth (cm) versus laser-derived rut depth (cm) and the linear model fitted to the data (red line).

Similarly, the linear mixed effect model indicates that the intercept, while varying across the test sites (Fig. 26), cannot be statistically proven to be different from zero. The test sites with clearly different than zero values for the intercept (Table 2, Fig. 26) were the ones where the errors were also the greatest. These test sites represented various conditions and the values were both under- and overestimated. The residuals of both models were normally distributed (Fig. 27).

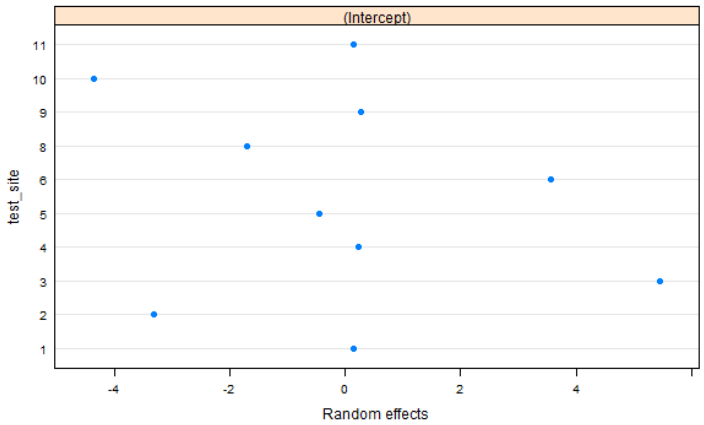

Figure 26. The plot of random effects of test site to the intercept.

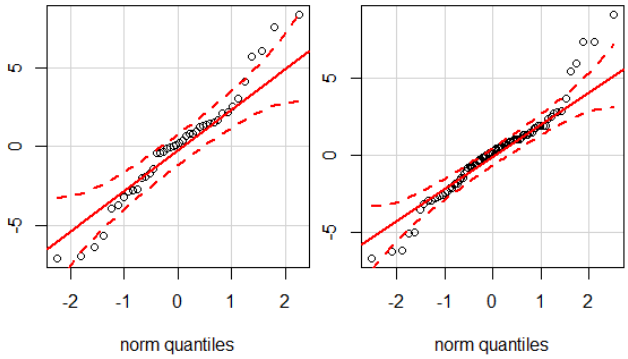

Figure 27. The residuals of linear model and linear mixed effect model are both normally distributed shown by the normal Q-Q plots.

The manually measured and laser-derived rut depths are explored in four test sites per rut "A" (Fig. 28) and "B" (Fig 29.) These show that in some test sites the laser and manually measured rut depths agree well (T1 for rut "A" and "B", T9 rut "A" 3rd pass) while in other there might be a slight locational errors (T3 rut "B" 5th pass, T9 rut "A" 2nd pass) or clear mismatches (T3 rut "A" 3rd pass, for example). The increase in rut depth after each pass is also captured on the test sites where it actually happened (T3, T6, and T9)

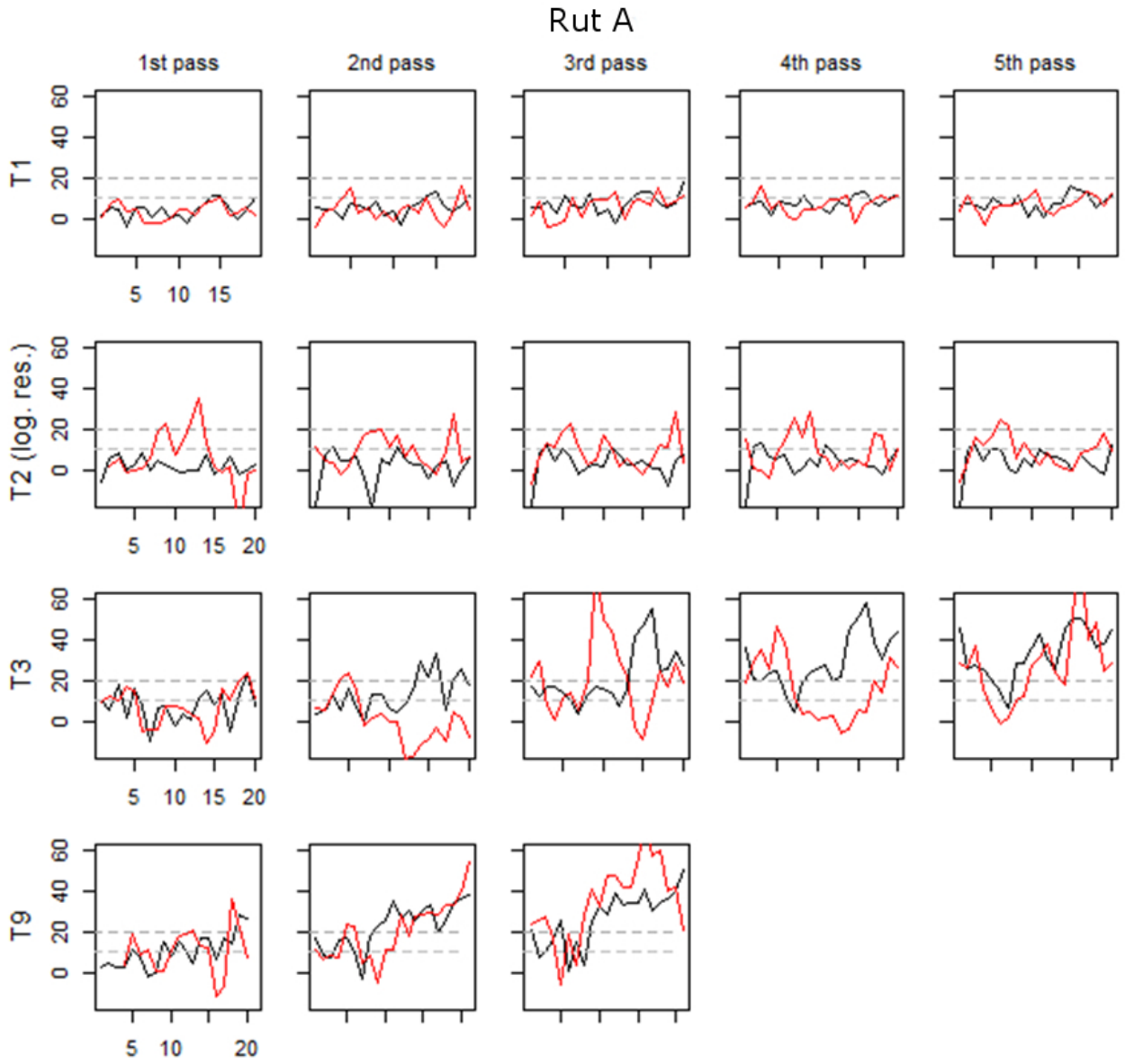

Figure 28. Manually measured rut depths (cm) (black line) and laser-derived rut depths (red line) on rut "A" in test sites T1, T2, T3, and T9. T2 was covered with logging residue. Test site T2 was covered with logging residue. The horizontal axis shows distance (m) from beginning of the test site.

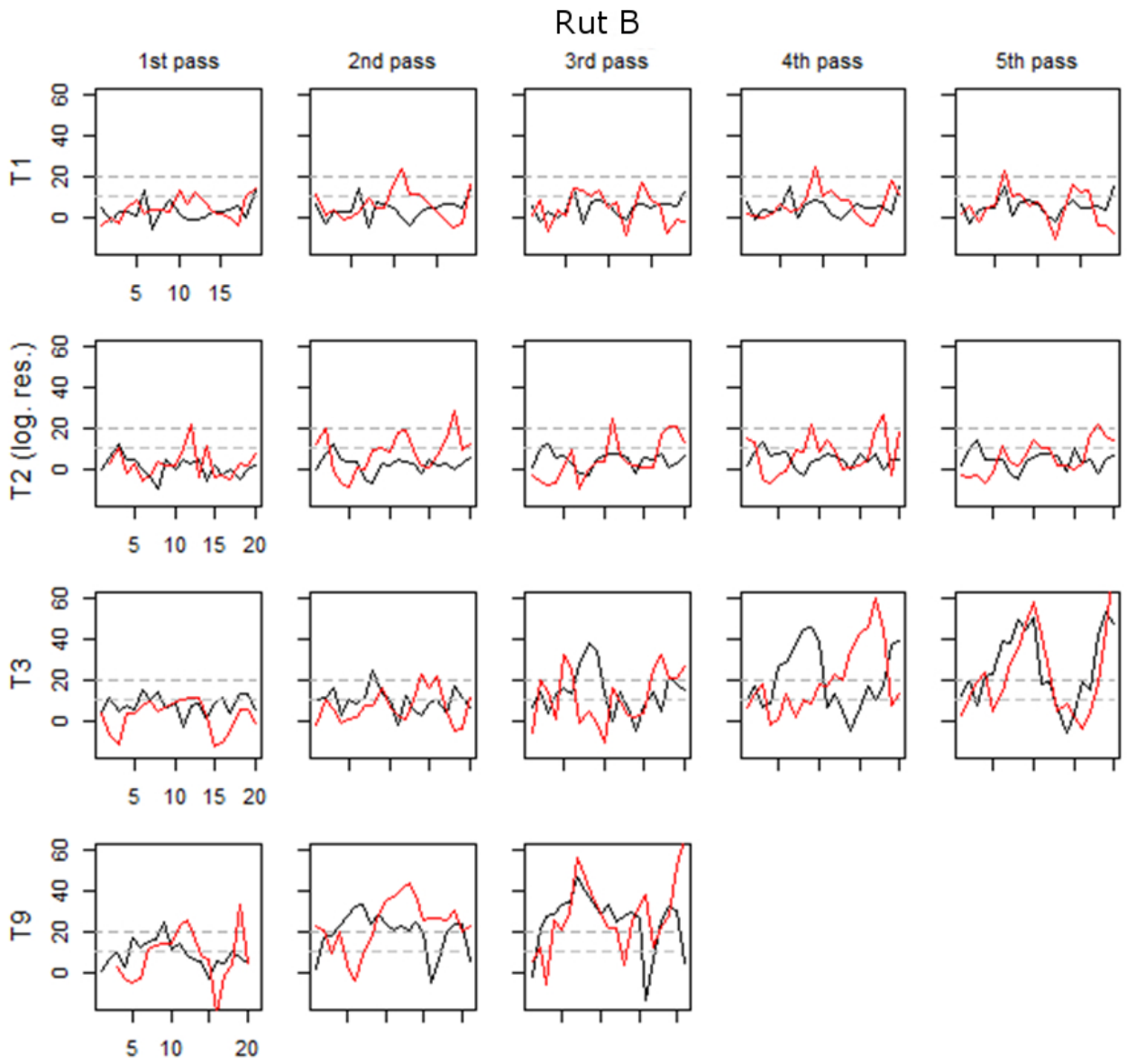

Figure 29. Manually measured rut depths (cm) (black line) and laser-derived rut depths (red line) on rut "B" in test sites T1, T2, T3, and T9. T2 was covered with logging residue. Test site T2 was covered with logging residue. The horizontal axis shows distance (m) from beginning of the test site.

2017 studies in Kuru in Central Finland

Results of LiDAR sensor, mounted directly downwards, were promising. Average rut depths of LiDAR and manual measurements are shown in Table 3 and Figure 30. According to initial analyses, RMSE of the laser predicted rut depths compared to reference measurements are at the level of 1.5 to2 cm.

Table 3. Mean rut depths of plots and differences in mean rut depths between manual and LiDAR measurements

		MANUAL					LIDAR				
Plot\Pass		2	3	4	5	6	2	3	4	5	6
131	mean	4.3	7.7	8.0	9.7	11.8	7.6	8.5	10.2	10.4	11.7
	dif in means						3.2	0.9	2.2	0.7	-0.1
132	mean	6.3	7.2	10.7	13.3	14.7	7.7	8.9	10.3	11.0	10.7
	dif in means						1.3	1.7	-0.4	-2.3	-3.9
133	mean	5.7	7.7	8.7	11.5	13.5	6.0	6.3	7.7	10.1	12.9
	dif in means						0.3	-1.3	-1.0	-1.4	-0.6
134	mean	9.0	10.2	11.7	14.3	17.7	8.9	11.3	13.0	14.6	16.4
	dif in means						-0.1	1.2	1.3	0.2	-1.3
141	mean	4.7	6.5	6.0	9.3	8.5	6.9	7.7	8.8	9.3	9.9
	dif in means						2.2	1.2	2.8	0.0	1.4
142	mean	3.8	5.7	6.0	8.2	7.2	5.8	6.0	6.7	7.4	7.9
	dif in means						1.9	0.3	0.7	-0.8	0.7
143	mean	2.2	5.2	5.5	7.5	8.5	2.6	4.7	6.1	6.9	7.4
	dif in means						0.4	-0.4	0.6	-0.6	-1.1
144	mean	4.8	6.3	5.7	6.8	7.7	6.0	8.0	9.1	9.8	10.5
	dif in means						1.1	1.7	3.4	2.9	2.9
151	mean	6.0	7.5	6.7	9.3	10.3	6.9	8.3	9.5	10.5	10.6
	dif in means						0.9	0.8	2.8	1.2	0.3
152	mean	5.0	9.8	8.7	11.2	11.5	5.8	7.2	8.5	9.6	9.9
	dif in means						0.8	-2.6	-0.2	-1.5	-1.6
153	mean	6.0	8.2	7.8	9.0	8.7	7.9	9.6	9.7	10.0	9.7
	dif in means						1.9	1.4	1.9	1.0	1.0
154	mean	4.5	8.0	7.8	9.2	11.0	7.4	6.0	6.9	7.5	12.2
	dif in means						2.9	-2.0	-0.9	-1.7	1.2
231	mean	8.2	10.2	12.0	14.3	14.8	-0.6	0.4	2.3	1.7	3.0
	dif in means						-8.7	-9.8	-9.7	-12.7	-11.8
232	mean	3.5	7.0	11.3	12.2	12.0	-0.5	0.9	-2.6	4.6	4.9
	dif in means						-4.0	-6.1	-13.9	-7.6	-7.1
233	mean	1.3	4.0	3.3	5.7	4.0	2.2	2.1	6.4	3.3	4.3
	dif in means						0.9	-1.9	3.1	-2.4	0.3
234	mean	6.2	8.2	9.8	12.0	11.5	4.9	6.3	2.5	10.2	10.9
	dif in means						-1.2	-1.8	-7.3	-1.8	-0.6
241	mean	3.0	5.2	5.2	5.2	5.8	6.8	7.5	7.8	9.0	8.6
	dif in means						3.8	2.3	2.7	3.8	2.8
242	mean	0.8	2.5	2.2	3.3	3.5	9.0	8.7	9.8	9.9	10.6
	dif in means						8.1	6.2	7.7	6.6	7.1
243	mean	4.2	7.0	6.7	8.7	8.8	4.5	5.9	6.9	8.1	7.6
	dif in means						0.4	-1.1	0.3	-0.6	-1.3
244	mean	4.3	5.8	5.2	7.3	8.2	2.1	3.2	3.7	4.2	4.6
	dif in means						-2.3	-2.6	-1.4	-3.1	-3.6
251	mean	4.2	5.5	5.0	6.2	6.7	3.2	5.0	4.7	5.6	6.3
	dif in means						-1.0	-0.5	-0.3	-0.6	-0.4
252	mean	5.3	5.8	6.2	8.8	9.0	5.7	6.5	7.8	8.4	8.8
	dif in means						0.3	0.7	1.6	-0.4	-0.2
253	mean	4.5	5.5	4.8	7.5	8.7	3.1	3.4	3.5	4.4	4.9
	dif in means						-1.4	-2.1	-1.3	-3.1	-3.8
254	mean	3.5	4.8	5.2	6.7	7.2	4.8	5.4	7.7	8.2	8.8
	dif in means						1.3	0.6	2.5	1.6	1.6

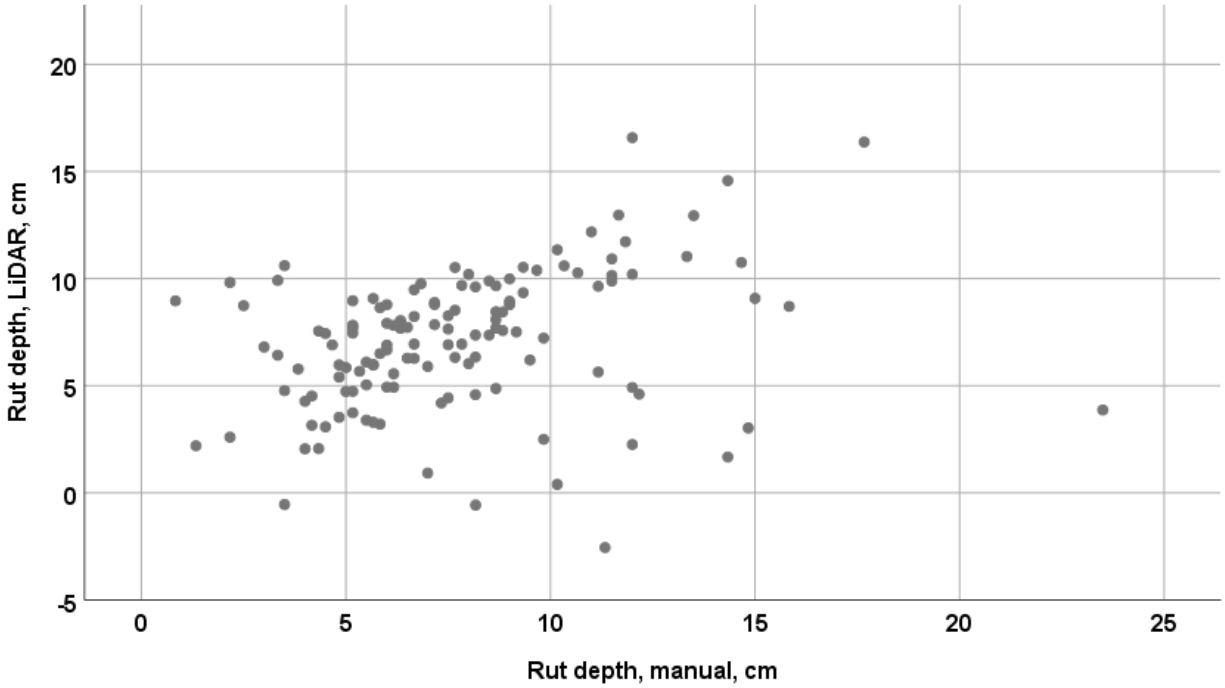

Figure 30. Scatter plot of LiDAR and manual measured results.

A rut depth map can already be produced directly from rut depth data including coordinates. Figure 31 shows an example from the test area return track to the actual test trails with traffic light type colour coding.

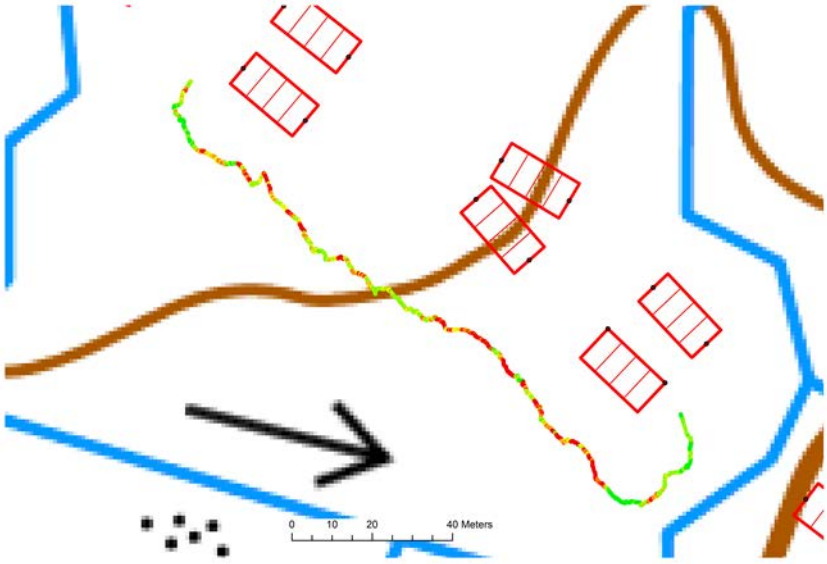

Figure 31. An example of a map produced by LiDAR rut measurement (green-yellow-red line) around study plot in Kuru test site.

Discussion

Based on our test results 2D-LiDAR could be reliable and effective tool for postharvest quality assessment, especially considering the the uncertainties related to manual measurements. Mounting the laser scanner to measure vertically improved measuring accuracy notably. At the logging site level are LiDAR measurement and GPS/Glonass positioning produces adequate results. Rut depth map can be easily produced from LiDAR measured dataset.

It seems that difficulties to measure the rut depth do not relate to the instrument *per se* but to the difficulty in defining the reference terrain level in an undulating forest environment. This concerns the manual measurements as well. Rocks and stumps between the wheels cause outlier values to the rut depth data and cutting debris outside the trail easily causes too deep rut depth values. In the simplified measuring system of the 2017 experiments these problems were solved by choosing 2% of the data representing the hits to the real soil surface.

Location information accuracy is one the key factors for laser scanner measurement method. Defining the exact location is challenging and while in operational applications we can forget about the need to match the laser-derived rut depths to the exact spots of manual measurements and concentrate in average rut depth values for sections of extraction trail with uniform depth class.

Several issues rise when considering the angle in which the laser scanner is mounted on the forest machine. Firstly, underestimation of rut depth can be brought by water gathering to the bottom of the rut. Especially, as the laser is in 45-degree angle and there is a few seconds between passing a point and measuring it. On the wettest of sites this is enough time for the water to find its way to the bottom of the rut. This is minimized with direct downward mounting of the laser scanner since the measurement occurs directly after the wheel has moved from the spot. Secondly, the slope is not considered in the rut depth calculations and this naturally affects the laser measurements as the angle varies along with tilting of the forest machine. This could be corrected, if we had a separate tilting sensor in the back of the forest machine, but in this study, the aim was to cope with as little extra instrumentation as possible. In addition, tilting and rocking of the machine caused that despite the 25 Hz measurement frequency of the laser scanner there were missing data range even to 50 cm lengths.

Mounting the scanner facing directly downward reduced the effect of slope and effect of tilting and rocking to the rut depth measurements and enabled the laser scanner to reach more accurate rut depth results. However, mounting the laser directly downward reduces the ability to use the data on the forest environment collected by the laser to other purposes, even though this information is not needed for the rut depth measurement. The value of mounting the laser scanner in 45-degree angle is in the ability to build the tree map

and measure location and speed independently of the forest machine CAN-bus data system. These additional measurements provide also a back-up for cases when data collection from CAN-bus system is for some reason obstructed.

LiDAR sensor was mounted simply at the end of the log on forwarder at the test drives. Installations for real forwarding need to be robust, but view for the sensor needs to be confirmed. Unobstructed view for the sensor is hard to maintain due to dust and mud in harvesting conditions. Mounting the laser scanner directly downward would mean that it should be mounted behind both wheels and preferably this should be done by the manufacturer, since it would need proper shields for the operational applications. Also, two laser scanners may be required since scanning both ruts may be difficult due to limited visibility when scanning directly downward. In mounting the laser scanner 45 degree angle, one scanner is enough since based on our results it seems that despite the right-side location of the laser on the forwarder there are matches and errors in the rut depths rather evenly (Fig. 28 and Fig 29, laser scanner was on top of rut: 3rd and 5th pass in rail “A” and 2nd and 4th pass in rail “B”).

Forest-machine mounted 2D-laser can provide a viable solution to be developed for collecting a large-scale rut depth data that is crucial for developing dynamic trafficability models and accurate predictions. Forestry machines represent a yet untapped resource as environmental data producer and this data can be crucial for ensuring sustainability in forest operations.

Plan for validation

The device is to be used in conjunction with future field studies. No further plans for validation in operational conditions within the Efforte project exist at the moment.